Ab Initio Quantum Mechanical Studies of the Kinetics and Mechanisms of Silicate Dissolution: H+ (H3O)+ Catalysis

ARTICLE *in* GEOCHIMICA ET COSMOCHIMICA ACTA · DECEMBER 1994

Impact Factor: 4.33 · DOI: 10.1016/0016-7037(94)90237-2

2 AUTHORS, INCLUDING:

Yitian Xiao
ExxonMobil
29 PUBLICATIONS **599** CITATIONS

Pergamon

Geochimica et Cosmochimica Acta, Vol. 58, No. 24, pp. 5379–5400, 1994

0016-7037/94 $6.00 + .00

0016-7037(94)00335-1

Ab initio quantum mechanical studies of the kinetics and mechanisms of silicate dissolution: $H^+(H_3O^+)$ catalysis

YITIAN XIAO and ANTONIO C. LASAGA
Department of Geology and Geophysics, Yale University, New Haven, CT 06511, USA

(*Received December* 4, 1993; *accepted in revised form August* 11, 1994)

Abstract—It is generally believed that the hydrolysis of Si—O—Si or Si—O—Al bonds is the key step in the dissolution processes of most silicates and aluminosilicates. High level ab initio molecular orbital calculations have been carried out to investigate the atomic processes of mineral dissolution by studying the following reactions:

$$\equiv Si-O-Si\equiv + H_2O \rightarrow \equiv Si-OH + \equiv Si-OH,$$

$$\equiv Si-O-Al\equiv + H_2O \rightarrow \equiv Si-OH + \equiv Al-OH,$$

$$\equiv Si-O-Si\equiv + H_3O^+ \rightarrow \equiv Si-OH + \equiv Si-OH_2^+,$$

$$\equiv Si-O-Al\equiv + H_3O^+ \rightarrow \equiv Si-OH + \equiv Al-OH_2^+.$$

Our ab initio results provide detailed molecular mechanisms, which can be used to explain the pH dependence of mineral dissolution rates, the formation of leached layers during feldspar dissolution, and recent experimental data on the kinetic isotope effect associated with quartz and feldspar dissolution. The hydrolysis reactions written above were studied by truncating the mineral surface so that a finite cluster of atoms could be used in the ab initio calculations. The potential energies involved in the adsorption of various aqueous species, as well as the reaction pathways leading to the formation of the transition state in each of the reactions, were then studied from first principles. The ab initio results indicate that: (1) The attack of $H^+(H_3O^+)$ onto the bridging oxygen site significantly weakens the Si—O—Si and Si—O—Al bridging bonds, (2) The calculated activation energies for the hydrolysis of Si—O—Si and Si—O—Al bonds by H_2O are 29 (32) kcal/mol and 26 (27) kcal/mol, respectively, while under H_3O^+ catalysis, they are 24 (22) kcal/mol and 16 kcal/mol (at the MP2/6-31G* level). Therefore, our ab initio results provide direct evidence of both H_3O^+ catalysis and of the preferred hydrolysis of Si—O—Al linkages over Si—O—Si linkages, and (3) Calculations show that pure H_2O hydrolysis leads to a rather big kinetic isotope effect (k_{H_2O}/k_{D_2O} = 2–4) while under H_3O^+ catalysis $k_{H_3O^+}/k_{D_3O^+}$ = 0.7–1.1. The latter results are in good agreement with recent experimental data for quartz and feldspar dissolution at low pH ($k_{H_3O^+}/k_{D_3O^+}$ = 1.1–1.3).

INTRODUCTION

DRIVEN BY IMPORTANT societal problems (e.g., acid rain, mineral resources, radioactive waste disposal, environmental pollution), geochemists have greatly advanced our knowledge of the thermodynamics and kinetics of mineral-fluid reactions in recent years. As a result of this work, great effort is now being spent on understanding the chemical and physical nature of mineral surfaces in contact with water. In coming to grasp the important steps such as hydration, adsorption, ion exchange, acid-base catalysis, and hydrolysis in mineral-water surface reactions, geochemists have come to rely on the tools of transition state theory (e.g., AAGAARD and HELGESON, 1982; HELGESON et al., 1984; MURPHY and HELGESON, 1987; DIBBLE and TELLER, 1981; KNAUSS and WOLERY, 1986, 1988; CASEY et al., 1988, 1989a,b, 1990; DOVE and CRERAR, 1990; DOVE and ELSTON, 1992; DOVE, 1994; BRADY and WALTHER, 1989, 1990; BLUM and LASAGA, 1988, 1991; NAGY and LASAGA, 1992; GRATZ and BIRD, 1993a,b). However, transition state theory can only be used in a very qualitative way if the molecular details of the reaction coordinate and the structure of the transition state are not known. It is clear that one of the central schemes in our understanding of heterogeneous kinetics is the elucidation of the important activated complexes and their modification by both surface properties and the composition of the solution near the surface as well as by temperature and pressure.

Among the most recent kinetic studies on silicate and aluminosilicate dissolution, an important task has been to understand the role that $H^+(H_3O^+)$ and OH^- play in catalyzing the reaction rates (which can vary over several orders of magnitude as a function of pH). Therefore, there has been increasing emphasis on the importance of adsorbed H^+ and OH^- complexes at the mineral-water interface on the overall kinetics of dissolution reactions. In fact, one of the great advances has been the establishment of a direct link between the dissolution rate and the amount of adsorbed H^+ and OH^- species, based on surface speciation modeling and surface titration experiments (FURRER and STUMM, 1986; BLUM and LASAGA, 1988, 1991; CARROLL-WEBB and WALTHER, 1988; BRADY and WALTHER, 1989; BRADY, 1992; DOVE and ELSTON, 1992; CASEY and SPOSITO, 1992). However, to try to understand the kinetics and mechanisms of silicate dissolution requires postulating the important molecular steps

leading to the adsorption of H^+ or OH^-, as well as the appropriate hydrolysis reactions. Deciding which steps are important, or even plausible, must ultimately depend on understanding the chemical bonding taking place on mineral surfaces. While the phenomenological treatments of adsorption have had to rely on operationally defined equilibrium constants and the introduction of several-layer models (extensions of the double layer) to describe the adsorption isotherms, these treatments are severely hampered by lack of information on the actual molecular processes governing the adsorption phenomena. Therefore, a first-principle investigation of the bonding and atomic nature of surface kinetics, including the types of activated complexes relevant to dissolution, and precipitation will clarify greatly the nature of mineral-fluid surface reactions.

High level ab initio calculations have been shown to be extremely successful in predicting the structures and physical properties of minerals (GIBBS, 1982; LASAGA and GIBBS, 1987, 1988, 1991; DOVESI et al., 1987). The important conclusion is that the major structures and energetics of silicates and oxides can be accounted for by short-range directional forces, or "covalent" bonding in the traditional sense (LASAGA and GIBBS, 1990, LASAGA, 1992). As a result, finite molecular clusters can be used to simulate the local environment and provide significant insights into the atomic forces and bonding pictures of minerals and glasses. With the vast increase in computational power, it is now feasible to calculate high level ab initio potential surfaces that incorporate bond-breaking and bond-forming processes. In particular, the reaction pathways and energetics of surface reactions involving oxides and silicates can be studied from the atomic point of view with these techniques (LASAGA and GIBBS, 1989, 1990; LASAGA, 1990, 1992; CASEY et al., 1990; KUBICKI et al., 1993).

The purpose of this study is to understand the atomic interactions responsible for the role of pH in the dissolution kinetics of silicates. The question addressed in this study can be summarized as follows: (1) What is the nature of H_2O and $H^+(H_3O^+)$ adsorption onto different active sites on the surfaces of minerals? (2) What is the mechanism of $H^+(H_3O^+)$ catalysis in the dissolution (hydrolysis) of silicates and aluminosilicates? To answer these questions, two prototype molecular clusters, $\equiv Si-O-Si\equiv$ and $\equiv Si-O-Al\equiv$, have been chosen to mimic the key linkages in silicates, e.g., quartz and feldspars. Furthermore, reactions with H_2O and $H^+(H_3O^+)$ have been incorporated to simulate the silicate dissolution processes. Calculations of the detailed atomic reactions, such as the adsorption and the hydrolysis processes, including the transition states have been conducted with ab initio methods. These calculations, in turn, provide the ability to extract many kinetic properties such as changes in activation energy, kinetic isotope effect, catalytic effect, temperature effect, and the overall rate law from first principles. These results are compared with previous experimental data (e.g., RIMSTIDT and BARNES, 1980; CHOU and WOLLAST, 1984; HELGESON et al., 1984; KNAUSS and WOLERY, 1986; SCHWEDA, 1989; BRADY and WALTHER, 1989, 1990; DOVE and CRERAR, 1990; CASEY et al., 1988, 1989a,b, 1990; BLUM and LASAGA, 1988, 1991; ROSE, 1991; GRATZ and BIRD, 1993a; DOVE, 1994).

COMPUTATIONAL METHOD

The ab initio calculations were carried out using Gaussian 90 (FRISH et al., 1990) on a DECstation 5000/200 at Yale University and the Cray-2 supercomputers at National Energy Research Supercomputer Center (NERSC), and Gaussian 92 (FRISH et al., 1992) on an IBM RISC/6000 350 at Yale University and the Cray Y-MP supercomputer at Florida State University Computing Center (FSUCC). Several extended basis sets, namely 3-21G*, 6-31G*, and 6-311G** (see HEHRE et al., 1986 for detailed description) were used. For the electron structure calculations, we employed restricted Hartree-Fock (HF) theory. Electron correlation is an important correlation to the HF results and was calculated by using second-order Møller-Plesset (MP2) perturbation theory. Possible problems, such as size consistency (HEHRE et al., 1986) or basis set superposition error (BSSE) (SAUER, 1989) were relatively negligible at the high level (e.g., MP2/6-31G*) of our ab initio calculations (MARTIN et al., 1989). Throughout most of the paper, numbers will be given that are based on calculations at the MP2/6-31G* level (unless otherwise stated). This level represents a rather robust calculation with an extensive basis set (the 6-31G* basis) and with the inclusion of the very important electron correlation correction (done using MP2 perturbation calculations).

The geometries of all stationary points are fully optimized at both HF and MP2 levels, with all the basis sets considered except for the MP2/6-311G** calculations. The transition states are obtained by requiring that one and only one of the eigenvalues of the Hessian (second derivative) matrix be negative and that the structure be a fully stationary point (i.e., all first derivatives of the energy with respect to any internal coordinate of any atom must be zero). The curvature of the potential surface in the neighborhood of each stationary point can be represented by the vibrational frequencies of the stationary structure. The vibrational frequencies and normal modes of all the stationary points are calculated using the second derivative matrix at the optimized geometry. The atomic structures, potential energies, and curvatures, thus calculated, were then used to calculate macroscopic kinetic properties for the mineral surfaces (e.g., the kinetic isotope effect; see LASAGA and GIBBS, 1990; CASEY et al., 1990).

MODELING MINERALS AND THEIR SURFACES

An important requisite of ab initio studies of minerals is to choose suitable molecular clusters to simulate the bulk solid or a solid surface, which enables much higher level quantum mechanical calculations to be carried out. Of primary concern is the size of the cluster and the basis set being used in such calculation. This is because the computing time increases dramatically with an increase in the size of the cluster as well as in the basis set. Therefore, both the chosen cluster as well as in the basis set should be big enough to accurately mimic the local environment of the structure of the mineral surface (compared with available experimental data), while small enough to assure computational feasibility.

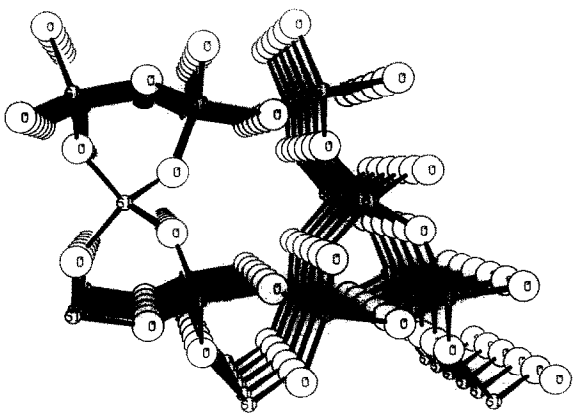

FIG. 1. Crystal structure of quartz.

The following pictures show the key steps used to model the infinite periodic structure of a mineral or a mineral surface with different sizes of molecular clusters. Figure 1 is the crystal structure of quartz, which has tetrahedral silicon units linked by bridging oxygens. Figure 2a–e represents a hierarchy of clusters used to mimic the local structure of quartz. Figure 2a is the $H_{12}Si_5O_{16}$ cluster, which contains five tetrahedral silicon units; Fig. 2b is the disilicic acid molecule $H_6Si_2O_7$, which has two full tetrahedral silicon units linked by a bridging oxygen; hydrogen atoms have been used here to terminate the linkages between those nonbridging oxygens and other network silicons. If we focus only on the Si—O—Si bond, without considering the nonlocalized effects, we can further truncate the linkages between the silicon atoms and the nonbridging oxygens in Fig. 2b with hydrogens; this truncation results in the disiloxane molecule cluster H_6Si_2O (Fig. 2c). Even smaller clusters are shown in Fig. 2d and e: the orthosilicic acid molecular cluster, H_4SiO_4, and the silanol molecule cluster, H_3SiOH,

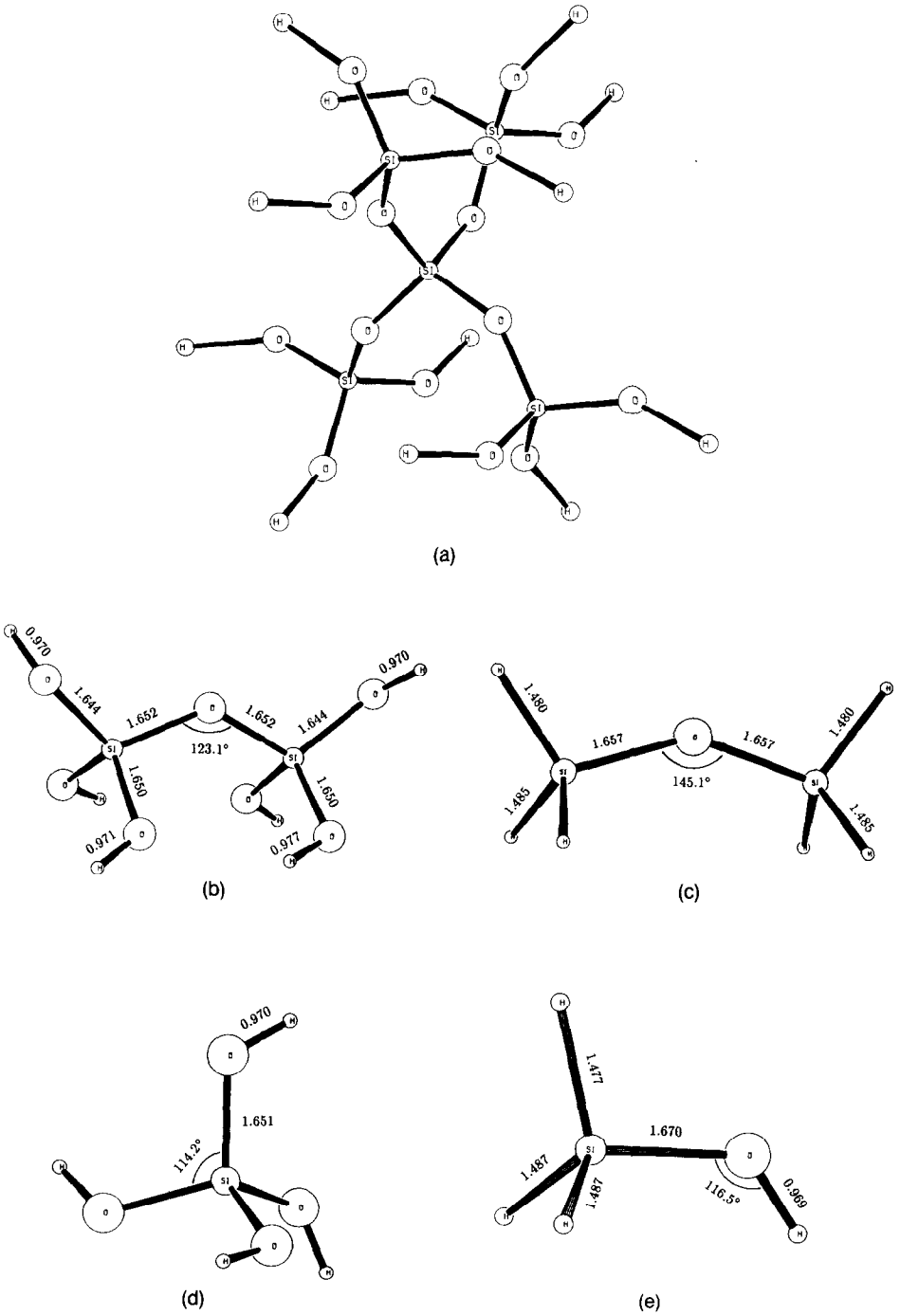

FIG. 2. Typical clusters used to mimic local structure of quartz: (a) $H_{12}Si_5O_{16}$ cluster which contains five silicon tetrahedral units; (b) Disilicic acid molecular cluster $H_6Si_2O_7$; (c) Disiloxane molecular cluster H_6Si_2O; (d) Orthosilicic acid molecular cluster H_4SiO_4, and (e) Silanol molecular cluster H_3SiOH. (b)–(e) are fully optimized geometries at the MP2/6-31G* level.

Table 1. Comparison of experimental bond lengths and angles for the Si–O–Si groups in gas phase and solid state molecular crystal siloxanes and silicates(after Gibbs (1982))

	R(SiO)Å	∠Si-O-Si(°)	Reference
H_6Si_2O (gas)	1.63	144	Almenning et al. (1963)
H_6Si_2O (solid)	1.63	142	Barrow et al. (1979)
Siloxane (solid)[a]	1.63	140	Newton and Gibbs (1980)
Silicates (solid)[a]	1.63	145	Geisinger and Gibbs (1981)
Silica glass[a]	1.62	152	Da Silva et al. (1975)
Alpha-quartz	1.61	144	Gibbs (1982)

[a] – Average value

respectively. Both of these clusters can be used to analyze the local behavior of the Si—O bond by replacing Si—O—Si with Si—O—H.

The structures shown in Fig. 2b–e are the optimized structures of the respective molecular clusters predicted at the MP2/6-31G* level. An important feature is the similarity in the geometry of these optimized structures to the experimental structure of the respective minerals. The geometric similarities have been noted by GIBBS (1982) and others and are indicative of the important role played by strong covalent (local) bonding. Therefore, very little difference exists between the size, shape, and bonding of a disiloxy (Si—O—Si) group in a solid silicate and those in a siloxane molecule. For example, the disiloxy group in the silicate α-quartz has an observed Si—O—Si bond angle of 144° and a SiO bond length of 1.61 Å (Table 1), which is in close agreement with a measured angle of 144° and a bond length of 1.63 Å in the gas phase disiloxane molecule H_6Si_2O. Such similarities also exist between solid siloxanes, silicates, and silica glasses. Our study, using clusters of different sizes, further demonstrates that important kinetic processes such as adsorption, hydrolysis, and acid catalysis during silicate dissolution are controlled by such local bonding, not by long-range forces involving numerous atoms.

Table 2 shows the dependence of optimized bond lengths and angles on basis set for the clusters $H_6Si_2O_7$, H_6Si_2O, H_4SiO_4, and H_3SiOH. The calculated SiO bond length at the HF level is slightly shorter than the experimental data, but addition of electron correlation leads to a predicted SiO bond length that is slightly longer than the experimental value. It is generally believed that such electron correlation is important in getting the correct bond length (HEHRE et al., 1986). Nevertheless, both HF as well as MP2 results are in close agreement with the corresponding experimental value in our case and we regard the MP2 results as the more accurate ones.

The value of the experimental Si—O—Si bond angle has a relatively broad range, with a mean value of 143°. The calculated Si—O—Si angles at the HF and MP2 levels for $H_6Si_2O_7$ show reasonable agreement. However, this is not true for H_6Si_2O. Calculations on H_6Si_2O at HF levels give quite obtuse Si—O—Si angles (i.e., 179.8 and 170.0° at 3-21G* and 6-31G*, respectively). A previous study for H_6Si_2O, based on HF/6-31G* (LASAGA and GIBBS, 1990) has predicted a reasonable Si—O—Si bond angle (143°), but a d orbital has been added to the bridging oxygen. With electron correlation included, the calculated Si—O—Si angles are 145.1 and 156° at MP2/6-31G* and MP2/6-311G**, respectively, giving better agreement with experimental value. NICHOLAS et al. (1992) argued that the Si—O—Si angle potential is highly anharmonic, with a very low (less than 1 kcal/mol) barrier to linearlization. This might account for the uncertainty of our calculations at the HF level. In addition, BURKHARD et al. (1991) reported that there were two conformations of $H_6Si_2O_7$, with Si—O—Si angles at 135 and 123°, respectively. However, only small basis sets (3-21G* and 3-21 + G*) were used in their calculations, and the result was shown to be sensitive to the basis set. Further higher level calculations with large basis sets and electron correlation are needed to confirm their

Table 2. Optimized geometries of various Si–O–Si(H) clusters at different level: bond length in angstroms and angle in drgrees, < > indicate average value

Cluster	Coordinate	HF/3-21G*	HF/6-31G*	MP2/6-31G*	MP2/6-311G**
$H_6Si_2O_7$	Si–O(br)	< 1.621 >	< 1.623 >	< 1.652 >	
	Si–O	< 1.618 >	< 1.625 >	< 1.650 >	
	O–H	< 0.962 >	< 0.948 >	< 0.972 >	
	∠Si-O-Si	< 134.0 >	131.8	123.1	
	∠Si-O-H	< 124.3 >	< 116.5 >	< 113.0 >	
H_6Si_2O	Si–O(br)	1.627	1.626	1.657	1.642
	Si–H	< 1.473 >	< 1.473 >	< 1.482 >	< 1.474 >
	∠Si-O-Si	179.8	170.0	145.1	156.5
H_4SiO_4	Si–O	< 1.620 >	< 1.628 >	< 1.651 >	< 1.643 >
	O–H	< 0.959 >	< 0.947 >	< 0.970 >	< 0.958 >
	∠Si-O-H	< 125.5 >	< 117.1 >	< 114.2 >	< 114.6 >
H_3SiOH	Si–O	1.633	1.647	1.670	1.659
	Si–H	< 1.473 >	< 1.473 >	< 1.482 >	< 1.474 >
	O–H	0.959	0.946	0.969	0.957
	∠Si-O-H	128.9	119.0	116.4	116.9

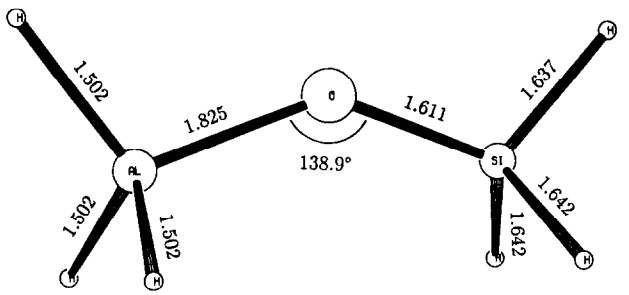

FIG. 3. H_6SiOAl cluster used to model the Si—O—Al linkages in aluminosilicates—fully optimized at MP2/6-31G*.

result. The importance of adding electron correlation to get the correct energetics, as well as vibrational frequencies, is even more obvious, as will be shown in a later section.

Figure 3 exhibits another important cluster, H_6SiOAl, which has been used to simulate the Si—O—Al linkages in aluminosilicates. Table 3 gives the optimized bond lengths and angles for the cluster H_6SiOAl as a function of basis set. The effects of the basis set, as well as electron correlation on the calculated geometry are quite similar to the ones described earlier for Si—O—Si. However, the Al—O bond length in H_6SiOAl is much longer than the Si—O bond length in H_6Si_2O, and concomitantly, the Si—O—Al bond angle is sharper than the Si—O—Si bond angle. There have been some debates about the selective hydrolysis of the Si—O—Al bond over the Si—O—Si bond in aluminosilicate dissolution (CAROL-WEBB and WALTHER, 1988; BRADY and WALTHER, 1989; BLUM and LASAGA, 1991; HELLMANN et al., 1990; WOLLAST and CHOU, 1992). From a kinetic point of view, the macroscopic dissolution rate is ultimately determined by the dynamics and atomic nature of the Si—O—Si and Si—O—Al linkages. Our high level ab initio calculations of the transition states and potential surface for the hydrolysis of Si—O—Si and Si—O—Al linkages will provide some first-principle answers to these questions.

AB INITIO STUDY OF ADSORPTION

H_2O Adsorption on Mineral Surface

Previous ab initio studies of H_2O adsorption onto silica and aluminosilicate surfaces (SAUER, 1987, 1989; GEERLINGS et al., 1984; HOBZA et al., 1981; MORTIER et al., 1984) have focused on the hydroxyl surface groups as the dominant adsorption site. Generally, most silica surfaces (amorphous or crystalline) contain approximately six OH groups/nm^2 (ILER, 1979). Adsorption of H_2O can occur at two particularly important OH groups, namely, the terminal OH and the bridging OH groups. Usually, the ab initio calculations of H_2O adsorption onto terminal OHs have used H_3SiOH or H_4SiO_4 clusters to simulate these surface sites (SAUER, 1987, 1989; GARRONE and UGLIENGO, 1989; UGLIENGO et al., 1990; LASAGA and GIBBS, 1989, 1990). DEJONG and BROWN (1980) carried out some of the very early studies of H_2O adsorption onto the bridging OH, using semiempirical calculations. The current ab initio methods can provide a more accurate quantitative treatment of both the adsorption of water and ions, as well as the following hydrolysis reactions at the surface of minerals.

As discussed by HOBZA et al. (1991), the reaction energies of more direct relation to the macroscopic enthalpy of adsorption of water onto silica surfaces measured in the laboratory, are the energy changes of the following reaction:

$$H_2O\cdots H_2O + M \Rightarrow M\cdots H_2O + H_2O \qquad (1)$$

or

$$(H_2O)_{n-1}\cdots H_2O + M \Rightarrow M\cdots H_2O + (H_2O)_{n-1}, \qquad (1a)$$

where M stands for the appropriate silica surface group. In other words, the energy gained in adsorbing the water must be weighted against the energy lost in breaking a hydrogen bond.

The calculated energies for reaction 1 must be corrected for zero-point energies of vibration to convert the energy changes to enthalpies, i.e.,

$$\Delta H_{0K} = \Delta E + \sum_i \frac{1}{2} h\nu_i^P - \sum_i \frac{1}{2} h\nu_i^R, \qquad (2)$$

where P and R stand for product and reactant, respectively. In Eqn. 1, one of the reactants is the water dimer, representing the water in solution. In Eqn. 1a, the model expands to look at one water molecule attached to several water molecules (e.g., 4, as in the water structure). The products then consist of the separated water dimer in one case, or the water cluster minus one water molecule in the other case and a water molecule adsorbed onto the cluster, M, representative of the mineral surface. Previous work has shown that the water dimer structure can be reproduced quite well by ab initio calculations (LASAGA, 1992).

The adsorption of a water molecule onto a terminal OH group can occur by either donation of a proton or reception of a proton. Previous studies (LASAGA and GIBBS, 1990; LASAGA, 1992) have shown that the most favorable mode of adsorption of water on silica is by "donor" adsorption onto a silanol group with $\Delta E = -3.5$ kcal/mol. The key step in silica dissolution, however, requires the acceptor adsorption of water onto disiloxane (LASAGA and GIBBS, 1990; LASAGA, 1992). This type of adsorption is necessary to form a new

Table 3. Optimized Geometries of Model Cluster H_6SiOAl as a Function of Basis Set

	HF/3-21G*	HF/6-31G*	MP2/6-31G*	MP2/6-311G**
Si—O	1.584	1.580	1.611	1.596
Al—O	1.769	1.794	1.825	1.809
Si—H^1	1.491	1.493	1.502	1.493
Si—H^2	1.491	1.493	1.503	1.493
Al—H^1	1.647	1.640	1.637	1.625
Al—H^2	1.647	1.644	1.642	1.630
∠Si-O-Al	180.0	153.9	138.9	149.5

* Distance in angstroms and angle in degrees

SiO bond between the oxygen of the water molecule and the surface silicon, a precursor to the hydrolysis of Si—O—Si bond. The ΔE for "acceptor" adsorption is calculated to be positive (0.22 kcal/mol), corroborating the hydrophobic nature of the dehydroxylated disiloxane-rich surface of silica.

Figure 4 shows the optimized geometry of water acceptor adsorption onto the larger H_6Si_2O disiloxane cluster. Once more, the calculated adsorption energies (Table 4) agree well with the results based on the smaller H_3SiOH silanol cluster (LASAGA and GIBBS, 1990; LASAGA, 1992). In other words, the adsorption details depend, to a very large degree, on the electronic structure surrounding the tetrahedral Si to which the water is adsorbing, and so the results are reasonably cluster-size-independent. The acceptor adsorption of water shown in Fig. 4 leads to a fivefold coordinated surface Si. The existence of fivefold coordinated Si in glasses and melts has been postulated in several molecular dynamics (MD) studies (ANGELL et al., 1988; KUBICKI and LASAGA, 1990) and inferred from recent spectroscopic work (XUE et al., 1989; POE et al., 1992). Although there are no mineral structures known to contain fivefold coordinated Si, there is both theoretical and experimental evidence for its existence. A recent ab initio study (KUBICKI et al., 1993) indicates that the fivefold coordinated Si may play a key role in silicate dissolution processes.

Note, that in Fig. 4 the distance from the Si to the oxygen of the adsorbed water molecule is 3.335 Å. It is interesting to point out that the OO distance in the channels along the c-axis of quartz is only around 3.56 Å. In other words, a water molecule would have to "squeeze" to adsorb within the spiral network of the silica tetrahedra (LASAGA, 1992). On the other hand, the original SiO bond length increases slightly upon the adsorption of the water molecule, from 1.657 to 1.678 Å, a precursor state to the ultimate rupture of the bond in the subsequent dynamics.

The adsorption of water onto Si—O—Al linkages (e.g., feldspars) can be studied similarly. The first point to note is

Table 4. Adsorption Energies — $H_6Si_2O + H_2O$ (Kcal/mol)

	ΔE^a	ΔE^b	ΔH^a_o	ΔH^b_o
HF/3-21G^* Adsorption				
Water Dimer	-10.95	-	-7.96	-
HF/6-31G^* Adsorption	-2.79	+2.81	-1.07	+2.40
Water Dimer	-5.60	-	-3.47	-
MP2/6-31G^* Adsorption	-6.16	+1.23	-4.19	+0.88
Water Dimer	-7.39	-	-5.07	-

a - energy change of $H_6Si_2O + H_2O = H_6Si_2O \cdots H_2O$
b - energy change relative to the water dimer formation

that the water adsorbs in only one configuration onto the Si—O—Al unit. In other words, there is no separate adsorption to the Si side or the Al side of the structure. This is a rather surprising result, which is repeated in the adsorption of H_3O^+ (see next section). Figure 5 shows this unique optimized geometry for water "acceptor" adsorption onto a H_6SiOAl cluster. The adsorption configuration has nearly equal distances between the oxygen of the incoming water and either the surface Si or the surface Al (3.605 Å vs 3.621 Å). Therefore, the H_2O can attack either the Si—O bond or the Al—O bond in a subsequent hydrolysis process.

Table 5 lists the calculated adsorption energies and enthalpies for water at an aluminosilicate surface site, based on different levels of the quantum mechanical calculations. Unlike the unfavorable acceptor adsorption of a water molecule onto the H_6Si_2O cluster, the negative adsorption enthalpies (e.g., ΔH_0 = -4.61 kcal/mol) indicate that Si—O—Al linkages in aluminosilicates favor water adsorption. Consistent with these energetics, the OH distance between the hydrogen of the adsorbed water and the bridging oxygen is 1.934 Å, shorter than the OH distance in water adsorption onto H_6Si_2O (2.016 Å). The favorable adsorption of H_2O on

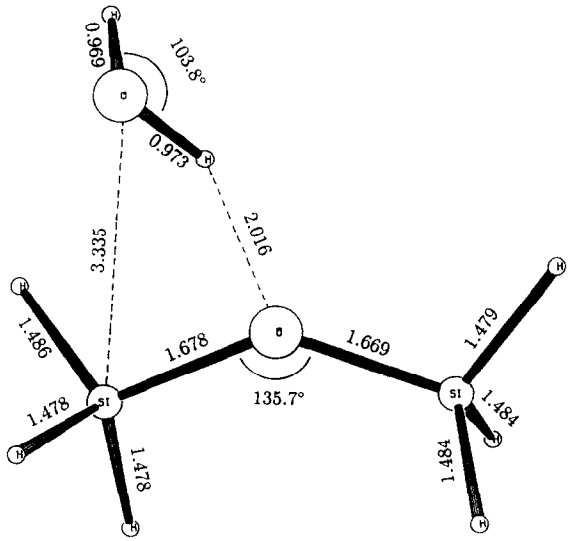

FIG. 4. Fully optimized geometry of the acceptor adsorption of water to the SiO bond of H_6Si_2O disiloxane cluster at MP2/6-31G*.

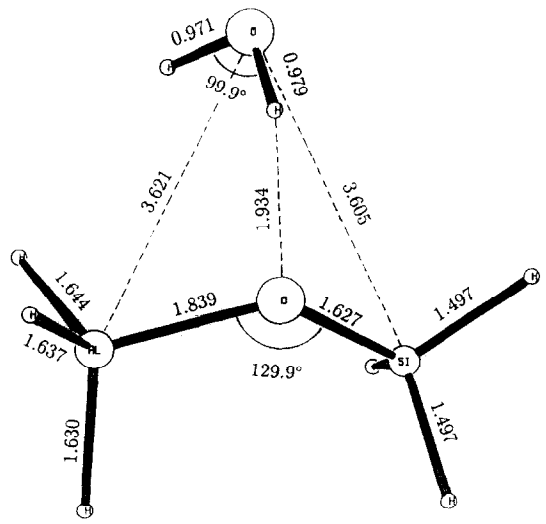

FIG. 5. Fully optimized geometry of the acceptor adsorption of water to the AlO(SiO) bond of the H_6SiOAl cluster at MP2/6-31G*.

Table 5. Adsorption Energies — $H_6SiOAl + H_2O$ (Kcal/mol)

	ΔE^a	ΔE^b	ΔH^a_o	ΔH^b_o
HF/3-21G* Adsorption	-14.10	-3.15	-11.57	-3.61
HF/6-31G* Adsorption	-11.69	-6.09	-9.23	-5.76
MP2/6-31G* Adsorption	-12.36	-4.97	-9.68	-4.61

a - energy change of $H_6SiOAl + H_2O = H_6SiOAl \cdots H_2O$
b - energy change relative to the water dimer formation

Si—O—Al over Si—O—Si may be part of the reason for the preferred hydrolysis of Si—O—Al linkages over Si—O—Si linkages.

Adsorption of H_2O onto a surface Al also leads to a five-coordinated Al. The existence of fivefold coordinated Al in SiO_2–Al_2O_3 glasses and liquids has been postulated by NMR and IR spectroscopy study and MD simulations (POE et al., 1992). Our ab initio study verifies the stability of AlO_5 moiety by obtaining a stable, fully optimized $Al(OH)_5^{2-}$ cluster. Similarly, such fivefold coordinated Al might play an important role in the dissolution processes of aluminosilicates.

$H^+(H_3O^+)$ Adsorption on Mineral Surfaces

To understand the acid and base catalysis of surface reactions, phenomenological models have been applied involving the equilibrium constants for the formation of adsorption complexes of H^+ and OH^- on the surface of minerals. The central scheme is to link the effect of acid and base on the dissolution rate of silicates to the acid-base behavior of the following surface reactions:

$$\equiv SiOH + H^+ \leftrightarrow \equiv SiOH_2^+, \quad (3)$$

$$\equiv AlOH + H^+ \leftrightarrow \equiv AlOH_2^+, \quad (4)$$

$$\equiv SiOH \leftrightarrow \equiv SiO^- + H^+, \quad (5)$$

$$\equiv AlOH \leftrightarrow \equiv AlO^- + H^+. \quad (6)$$

The equilibrium constants for these reactions can be established by surface titration experiments which, in turn, enable a bulk speciation calculation to be performed for the species on the mineral surface in a similar fashion to the speciation calculations carried out for aqueous solution. The dissolution rate of silicates has then been linked to the amount of adsorbed H^+ or OH^- species and a rate law (e.g., WIELAND et al., 1988; STUMM and WOLLAST, 1990; DOVE and ELSTON, 1992) can be simply written as

$$\text{Rate} = k_1(SiOH_2^+)^{n_1} + k_2(SiOH)^{n_2} + k_3(SiO^-)^{n_3}, \quad (7)$$

where k_1, k_2, and k_3 are rate constants and $SiOH_2^+$, SiOH, and SiO^- stand for the concentrations of positively, neutrally, and negatively charged surface species, respectively. However, "species" such as $SiOH_2^+$ include any kind of possible adsorption species which are positively charged. For example, it is commonly agreed that the attachment or detachment of a proton onto a silanol group is an important process for the bulk adsorption of H^+. A similar point has been made by HIEMSTRA et al., (1989a,b) who argue that a single equilibrium constant for adsorption reactions on mineral surfaces such as reactions 3–6 is too simplistic. They stress the fact that various surface groups should be distinguished on the surface of minerals including variations in the coordination of the metal. Surface titrations cannot distinguish between the various adsorption sites and among the different coordination numbers.

One can study the adsorption and desorption of H^+ onto silanol groups using the following clusters: $H_3SiOH_2^+$, H_3SiOH, and H_3SiO^-. Figure 6 exhibits the optimized geometries of these clusters. However, since the general dissolution mechanism requires the detachment of silica tetrahedra, a kinetically important adsorption of protons is to the bridging oxygen in siloxane Si—O—Si groups (LASAGA, 1990, 1992; DOVE, 1994). Figure 7 illustrates the marked structural changes in the siloxane group induced by the attachment of a proton onto the bridging oxygen. In particular, the much elongated SiO bonds will result in a strongly modified reaction surface for the hydrolysis reaction.

SAUER (1987) studied the relative acidities of various OH surface groups, and his results indicate that the pK of the H^+ on a bridging oxygen is much smaller than that of the terminal hydroxyl, i.e., the bridging hydrogen is a much more acidic hydrogen. Therefore, the population of hydrogens on bridging

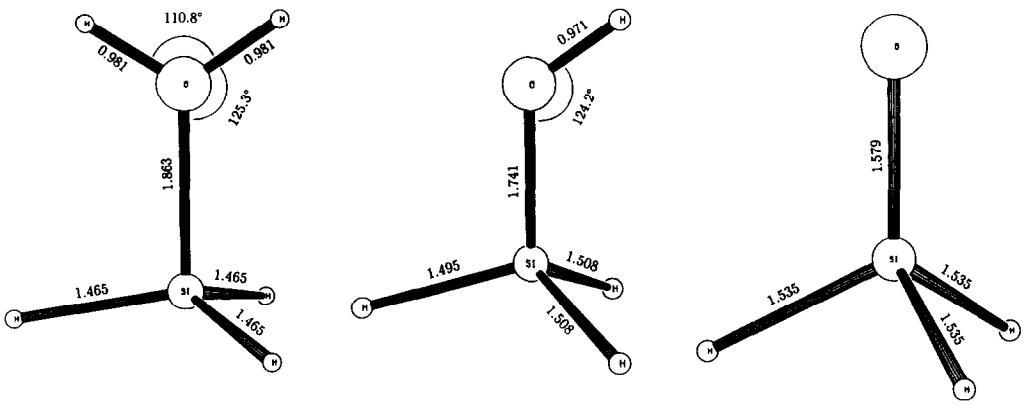

FIG. 6. Clusters used to model positively, neutrally, and negatively charged surface silanol groups. (a) $H_3SiOH_2^+$, (b) H_3SiOH, and (c) H_3SiO^-. Geometries optimized at MP2/6-31G*.

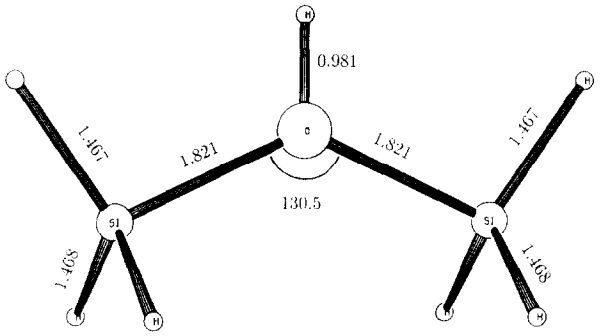

FIG. 7. Cluster used to investigate the effect of H^+ adsorption on Si—O—Si linkages in silica. Compare with Fig. 2c for the unperturbed disiloxane structure and note the elongated SiO bond in the H^+ adsorbed complex. Geometries optimized at MP2/6-31G*.

oxygens are expected to be small at the typical pHs of acidic solutions. However, it is important to point out that the rates of many chemical reactions are usually controlled by reactive intermediates, which may not necessarily be the dominant adsorbed species. Therefore, the actual mechanism of dissolution may be controlled by the adsorption of H^+ onto sites such as the bridging oxygens in framework silicates. The hydrolysis rate at these sites may be increased so much that the overall rate is controlled by these infrequent adsorption sites.

Now an interesting question arises: what is the different role for H^+ and H_3O^+ in the acid catalyzed dissolution processes? In other words, what is the structural distinction between H^+ attack on a bridging oxygen followed by water adsorption and direct H_3O^+ attack on a bridging oxygen? These questions can be answered by performing two calculations: (1) putting an optimized water molecule on top of an optimized disiloxane which has a proton adsorbed on the bridging oxygen site, then fully optimizing the whole system (Fig. 8), and (2) putting an optimized H_3O^+ molecule (Fig. 9) on top of an optimized disiloxane, then fully optimizing the whole system. The energy monotonically decreases towards the minimum as the H_3O^+ approaches the disiloxane and finally, the stable adsorbed species forms with one of the H atom from hydronium transferred to the bridging oxygen site in the disiloxane. In the end, we get exactly the same configuration as we obtained in the first calculation. This indicates that there is no distinction between H^+ + water and H_3O^+ (for example, if an additional minimum geometry with the adsorbed H^+ separated from the water was found then there would be a dynamical distinction). Note that, ultimately, the adsorption of H_3O^+ is the important entity, because kinetically, for any hydrolysis, we need the water molecule present, not just a proton as in H^+.

Similar to the study of the energetics of water adsorption on a silica surface, an appropriate reaction to use in studying the energetics of H_3O^+ adsorption onto a silica surface is

$$H_2O\cdots H_3O^+ + M \leftrightarrow M\cdots H_3O^+ + H_2O, \quad (8)$$

where M stands for silica surface groups such as disiloxane. In other words, the energy gained in adsorbing the hydronium must be weighted against the energy lost in breaking a H bond between a hydronium and a water. The calculated ΔH_0

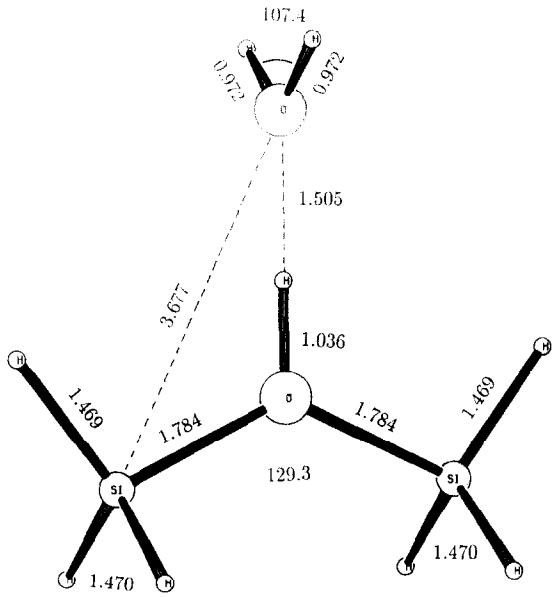

FIG. 8. Fully optimized MP2/6-31G* geometry for the adsorption of water onto a H^+ catalyzed disiloxane group (= adsorption of hydronium ion onto an unperturbed disiloxane; note the hydrogen transfer from hydronium ion to the bridging oxygen of disiloxane).

for the reaction,

$$H_3O^+ + H_2O \leftrightarrow H_3O^+\cdots H_2O, \quad (9)$$

is 38.47 kcal/mol (Table 6), which is in good agreement with experimental value, 36 kcal/mol (YAMABE and MINATO, 1984). Figure 10 exhibits the optimized geometry of the water-hydronium dimer (the product of reaction 9). The calculated OO distance, 2.42 Å, also agrees well with the experimental value of 2.52 Å (YAMABE et al., 1984).

The calculated adsorption energy for the adsorption of a hydronium ion onto disiloxane predicts an energetically favorable adsorption, i.e., the enthalpy change for the reaction

$$H_2O\cdots H_3O^+ + H_6Si_2O = H_6Si_2O\cdots H_3O^+ + H_2O \quad (10)$$

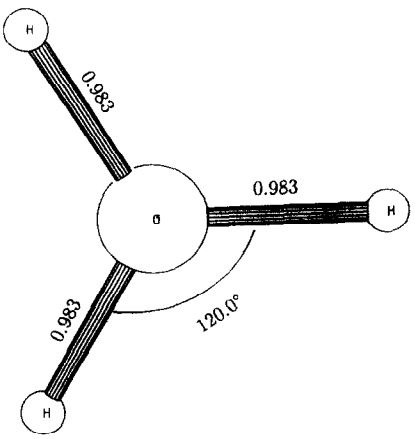

FIG. 9. Fully optimized geometry of H_3O^+ hydronium ion at MP2/6-31G*.

Table 6. H_3O^+-H_2O Dimer Formation

	HF/3-21G*	HF/6-31G*	MP2/6-31G*	ΔE^{expt}
ΔE	-52.56	-34.62	-40.35	
ΔE_{ZEC}	2.60	2.67	1.88	
ΔH_o	-49.98	-31.95	-38.47	-36.0[a]

a - Yamabe et al., 1984

Table 7. Adsorption Energies — $H_6Si_2O + H_3O^+$ (Kcal/mol)

	ΔE^a	ΔE^b	ΔH_o^a	ΔH_o^b
HF/3-21G* Adsorption	-36.21	+16.25	-35.08	+14.90
H_3O^+-H_2O Formation	-52.56	-	-49.98	-
HF/6-31G* Adsorption	-39.41	-4.79	-36.94	-4.99
H_3O^+-H_2O Formation	-34.62	-	-31.95	-
MP2/6-31G* Adsorption	-43.79	-3.44	-42.34	-3.87
H_3O^+-H_2O Formation	-40.35	-	-38.47	-

a - energy change of $H_6Si_2O + H_3O^+ = H_6Si_2O \cdots H_3O^+$
b - energy change relative to the H_3O^+-H_2O Formation

is negative, $\Delta H_0 = -3.87$ kcal/mol (Table 7). This favorable adsorption energy is in contrast to the unfavorable adsorption energy for the adsorption of water onto disiloxane ($\Delta H_0 > 0$). The result suggests that the silica surface favors the adsorption of H_3O^+ over H_2O.

Figure 11 is the cluster used to investigate the effect of H^+ adsorption on Si—O—Al linkages in feldspars. Notice that, after adsorption of H^+ onto the bridging site, both AlO and SiO bonds have been significantly elongated. Figure 12 gives the optimized geometry of H_3O^+ adsorbed on the H_6SiOAl cluster, which leads to similar elongation in the AlO and SiO bonds. Table 8 lists the calculated adsorption energies and enthalpies of the adsorption process at different levels, and shows that the adsorption energies for H_3O^+ are more negative than those for the corresponding H_2O adsorption onto H_6SiOAl. The favorable adsorption of H_3O^+ over H_2O on both Si and Al sites should play a role in the catalysis of surface reactions in aluminosilicates by acids.

AB INITIO STUDIES OF MECHANISMS OF SILICATE DISSOLUTION KINETICS

Understanding the reaction kinetics at surfaces requires (1) a particular elementary reaction sequence, (2) the transition states involved in each elementary reaction of the sequence, and (3) the potential surface leading from reactants to transition state and then to products (this includes a normal mode analysis of the motion along the reaction coordinate near the transition state).

In this section, we will apply this procedure to four reaction mechanisms. Because surface reactions involving both silicates and aluminosilicates are of great interest, two key surface structural units will be studied: Si—O—Si and Al—O—Si, where each Si or Al atom is in a tetrahedral environment. These linkages form the basis for the framework of many silicates and aluminosilicates. In dissolution reactions, we postulate that it is the breakdown of these units that controls the overall rate. Therefore, we will propose reaction mechanisms involving these two units. In addition, mineral reactions in aqueous media involve not only the action of water molecules, but also the important catalytic effect of either H^+ or OH^- ions. Therefore, two different reaction mechanisms will be studied for each of the structural units; one mechanism involves hydrolysis with water and the other mechanism involves the hydrolysis reaction by water in the presence of the H^+ ion on the surface. After discussing the ab initio results, this section will end with a comparison to known experimental data on mineral-water kinetics.

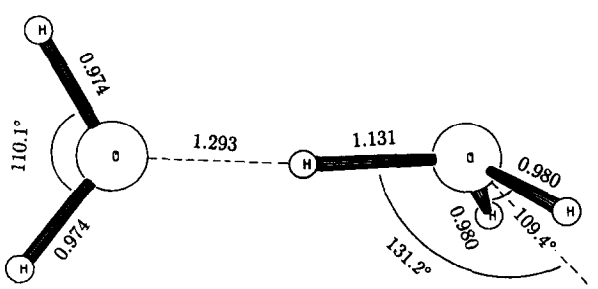

FIG. 10. Fully optimized geometry of the water-hydronium dimer at MP2/6-31G*.

Transition State of the Hydrolysis Reactions

H_2O hydrolysis of the Si—O—Si surface unit

The activated complex for the hydrolysis reaction of quartz has been studied by LASAGA and GIBBS (1989, 1990) and CASEY et al. (1990). These papers, however, used small clusters and did not, generally, include electron correlation with a large basis set. Our calculations are based on the H_6Si_2O cluster and use a large basis set, 6-31G*, with electron correlation included at the second-order Møller-Plesset perturbation level (MP2/6-31G*). The optimized geometry of the transition state for the hydrolysis reaction involving H_2O is shown in Fig. 13.

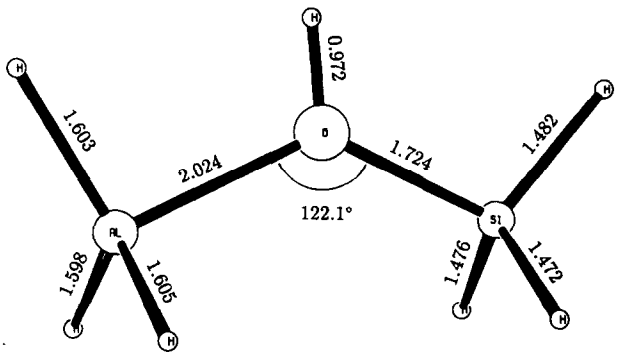

FIG. 11. Cluster used to investigate the effect of H^+ adsorption on Si—O—Al linkages in feldspar. Compare with Fig. 3 for the unperturbed H_6SiOAl structure; note the elongated AlO bond in the H^+ adsorbed complex. Geometries optimized at MP2/6-31G*.

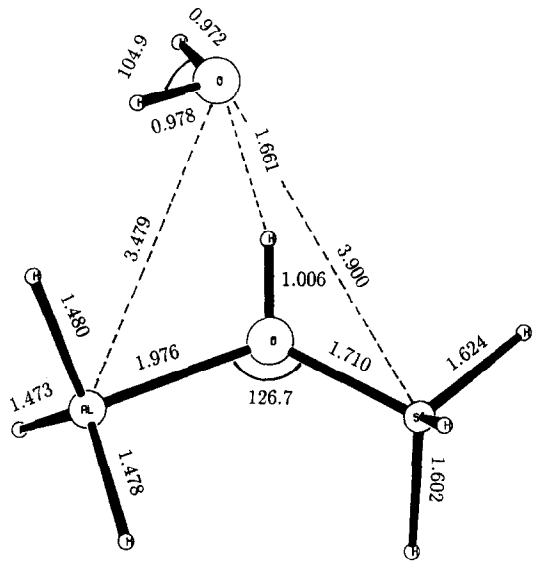

FIG. 12. Fully optimized MP2/6-31G* geometry for the adsorption of water onto a H^+ catalyzed H_6SiOAl group (= adsorption of hydronium ion onto an unperturbed H_6SiOAl, notice the hydrogen transfer from hydronium ion to the bridging oxygen of H_6SiOAl).

Besides the geometry of the activated complex, a very important kinetic feature is the actual pathway that links reactants and products through the activated complex. This pathway is termed the reaction coordinate. Once the transition state has been found, an analysis of the normal mode of the activated complex which has the negative eigenvalue (i.e., the imaginary frequency) can be carried out. This normal mode coincides with the reaction coordinate for the hydrolysis reaction in the neighborhood of the activated complex. One can analyze this normal mode by distorting the molecular geometry of the transition state by the cartesian coordinate vector corresponding to the particular normal mode and observing which internal coordinates change (see LASAGA and GIBBS, 1989, 1990; LASAGA, 1992). The internal coordinate analysis of the reaction coordinate near the transition state for the hydrolysis of H_6Si_2O by H_2O is given in Table 9. Only the relative changes of bond lengths and angles that change significantly are shown in the table. Note that the normal mode along the reaction coordinate increases the $O^{water}H$ distance and decreases the $O^{bridge}H$ distance from the corresponding value at the transition state geometry. This analysis indicates that motion along the reaction coordinate in-

Table 8. Adsorption Energies — $H_6SiOHAl + H_2O$ (Kcal/mol)

	ΔE^a	ΔE^b	ΔH_o^a	ΔH_o^b
HF/3-21G* Adsorption	-27.06	-16.11	-23.86	-16.90
HF/6-31G* Adsorption	-14.10	-8.50	-11.09	-7.62
MP2/6-31G* Adsorption	-18.06	-10.67	-15.09	-10.02

a - energy change of $H_6SiOHAl + H_2O = H_6SiOHAl \cdots H_2O$
b - energy change relative to the water dimer formation

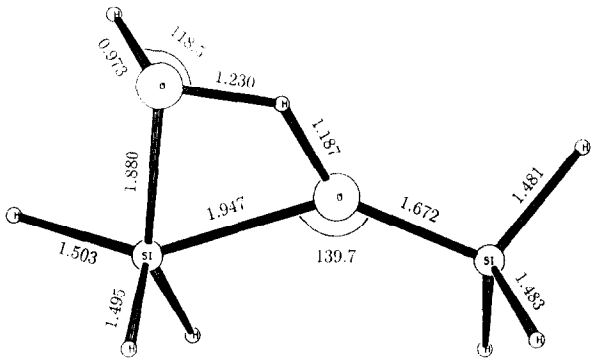

FIG. 13. Fully optimized geometry of the transition state for the hydrolysis reaction of water on a disiloxane group at MP2/6-31G*.

volves predominantly the transfer of the H atom from the water molecule to the bridging oxygen of the Si—O—Si site. Interestingly, the two long SiO bonds (which ultimately must also get involved in the reaction) are not very active in the reaction coordinate normal mode. Our new result is in excellent agreement with previous ab initio studies at lower level (LASAGA and GIBBS, 1989, 1990; LASAGA, 1992) and verifies the statement that the H transfer dominates the hydrolysis reaction in this mechanism. According to such analysis, there will be a large kinetic isotope effect as well as a nontrivial tunneling effect for the hydrolysis of Si—O—Si bonds.

Using the optimized geometries of the reactants and the activated complex, the activation energy, $\Delta E^{\ddagger}$, can be obtained as the energy difference between the activated complex and reactants. The calculated activation energies for the hydrolysis of disiloxane using different basis sets with and without electron correlation are listed in Table 10. Electron correlation has been shown to be very important in obtaining accurate activation energies. For example, $\Delta E^{\ddagger}$ drops from 45.90 kcal/mol at HF/6-31G*, to 31.98 kcal/mol at MP2/6-31G*, in this case.

To compare the calculated energy changes to experimental quantities the zero-point vibrational energies must be included,

$$\Delta H_0^{\ddagger} = \Delta E^{\ddagger} + \sum_{i=1}^{3N-7} \frac{1}{2} h\nu_i^{\ddagger} - \sum_{i=1}^{3N-6} \frac{1}{2} h\nu_i^{\text{ads}}. \qquad (11)$$

This correction is nontrivial and reduces the energy barrier by 2.05 kcal/mol for the hydrolysis of disiloxane. Note that part of the loss in the barrier is due to the fact that the activated complex is "loose" compared to the adsorption complex (see Figs. 4, 13). Structures with many elongated bonds tend to have lower frequencies of vibration and hence, smaller $\frac{1}{2}h\nu$ corrections. Therefore, the increase in zero-point energy of vibration is bigger for the stable adsorption complex than for the activated complex. This correction has important consequences for the kinetic isotope effect (LASAGA and GIBBS, 1990; CASEY et al., 1990).

Because finite clusters are being used to simulate surfaces containing many atoms, it is essential to investigate the effect of cluster size on the various calculated properties. Therefore, similar calculations have been carried out on different clusters

Table 9. Reaction Coordinate normal mode for the H_6Si_2O - H_2O transition state — MP2/6-31G* result (ν = 1084 i)

Internal Coordinate[a]	Stationary Point[b]	Normal Mode Value[c]
SiO bond	1.974 Å	1.971 Å
SiO bond	1.880 Å	1.884 Å
OH[d] bond	1.187 Å	1.357 Å
OH[d] bond	1.230 Å	1.056 Å
H[e]OH[d] angle	118.5°	114.3°
SiOH[d] angle	78.6°	74.9°

a - only internal coordinates that involve in reaction are listed
b - see geometry in figure 13
c - value of internal coordinate after vibration is allowed
d - H atom being exchanged in figure 13
e - H atom (unreactive) in water molecule

such as H_3SiOH, $H_2Si(OH)_2$, H_4SiO_4, H_6Si_2O, and $H_6Si_2O_7$, to study the hydrolysis of Si—O—Si and Si—O(H) linkages. The calculated transition states for the hydrolysis of H_3SiOH, $H_2Si(OH)_2$, H_4SiO_4, and $H_6Si_2O_7$ by H_2O are shown in Fig. 14a,b,c, and d, respectively. Table 11 compares the calculated activation energies derived from these different clusters. Note that the calculated local structures of the transition states and the activation energies based on H_6Si_2O, H_3SiOH, $H_2Si(OH)_2$, H_4SiO_4, as well as $H_6Si_2O_7$ are almost the same. This strong similarity supports the validity of using small clusters to mimic the local environment of silicates as well as the atomic dynamics leading to the relevant surface reactions.

H_2O Hydrolysis of the Si—O—Al Surface Unit

The hydrolysis reaction of the Si—O—Al bond is a key step in the dissolution of aluminosilicates (e.g., feldspars). Figure 15 shows the fully optimized structure of the transition state for the hydrolysis of the H_6SiOAl cluster. The calculated $\Delta E_a^{\ddagger}$ and $\Delta H_0^{\ddagger}$ for this hydrolysis are summarized in Table 12.

The normal mode analysis of the reaction coordinate for the hydrolysis of H_6SiOAl is shown in Table 13. First of all, this transition state has a much lower imaginary frequency (198.1 i cm^{-1}) than the transition state for the hydrolysis of H_6Si_2O (1084 i cm^{-1}). Hydrogen transfer is, once more, an important component of the normal mode along the reaction coordinate. However, in this case, the normal mode also has a significant component that involves changes in the Al—O bond length. For example, in this motion of the normal mode, the Al—O bond length varies from 1.446 Å at the stationary point to 1.353 Å at the normal mode. The Si—O bond does not seem to change as much during the normal mode motion near the transition state configuration. These differences will have important consequences on the kinetic behavior.

Transition State of the Hydrolysis Reaction Under $H^+(H_3O^+)$ Catalysis

Because the dissolution rates of most minerals are pH dependent, it is generally assumed that one of the reactants involved in the rate-determining step of mineral hydrolysis are H^+ and OH^- or their adsorbed equivalents. The effect of $H^+(H_3O^+)$ adsorption on the structures and energetics of Si—O—Si and Si—O—Al linkages needs to be extended, then, to investigate the transition state of the hydrolysis reaction in the presence of $H^+(H_3O^+)$.

H_3O^+ Hydrolysis of the Si—O—Si Surface Unit

Figure 16 illustrates the transition state for the hydrolysis of H_6Si_2O disiloxane under $H^+(H_3O^+)$ attack. The calculated $\Delta E_a^{\ddagger}$ and $\Delta H_0^{\ddagger}$ are summarized in Table 14. The interesting

Table 10. Hydrolysis Transition State — $H_6Si_2O + H_2O$ (Kcal/mol)

	HF/6-31G*	MP2/6-31G*//6-31G*	MP2/6-31G*	ΔE^{expt}
$\Delta E_a^{\ddagger}$	45.90	32.31	31.98	
ΔE_{ZEC}	-1.42	-1.42	-2.05	
ΔH_o	44.53	30.89	29.93	16-21[a]

a - Rimstidt and Barnes, 1980; Dove and Crerar, 1990; Dove, 1994

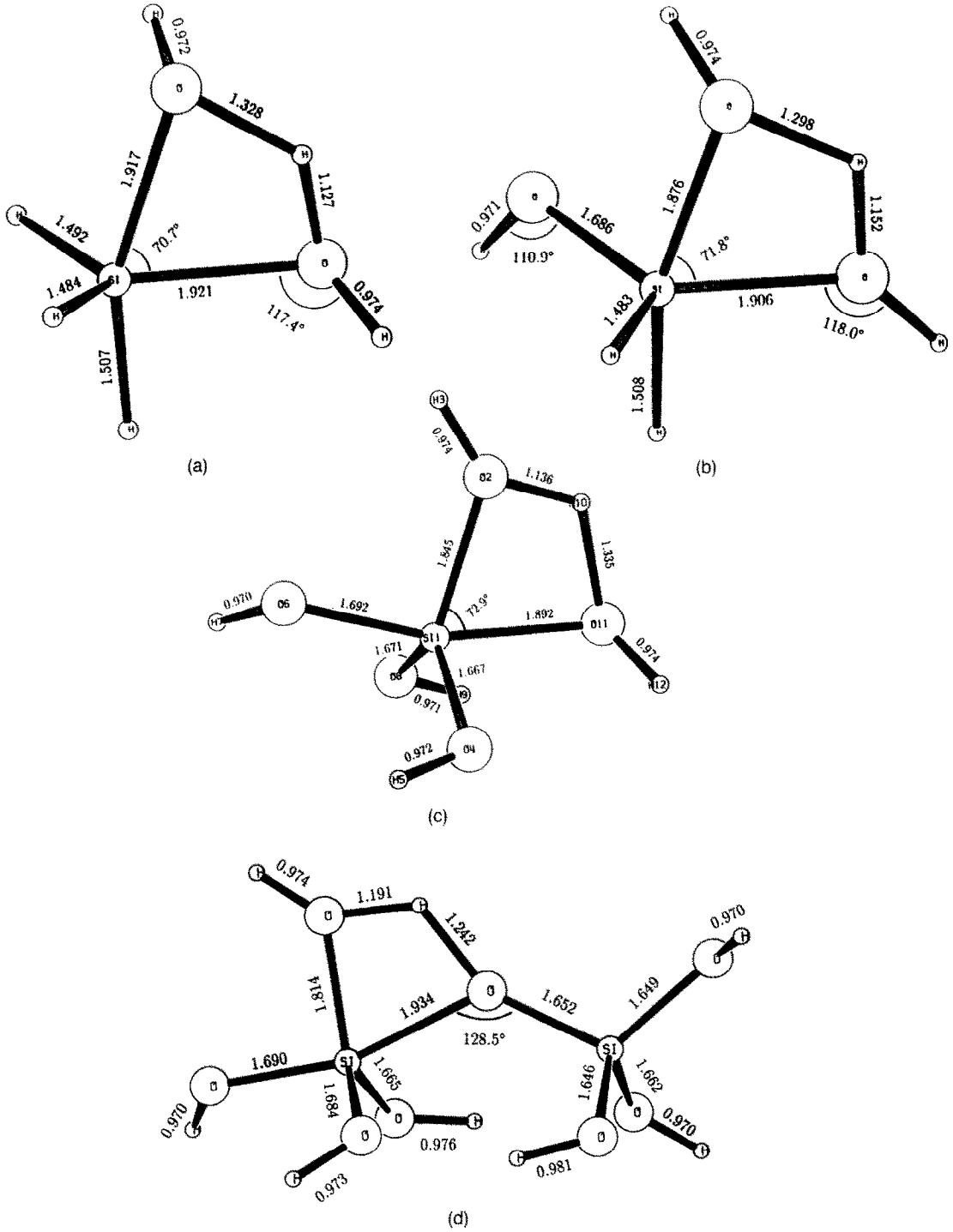

FIG. 14. Fully optimized MP2/6-31G* geometries of the transition states for the hydrolysis reaction of water on a) H_3SiOH; b) $H_2Si(OH)_2$; c) H_4SiO_4; and d) $H_6Si_2O_7$.

results of this new calculation are the dramatic change of the configuration of the transition state, as well as the big decrease in $\Delta E_a^{\ddagger}$ (compare Tables 9 and 14) from previous calculations. For example, the activation energy for the hydrolysis of disiloxane is 31.98 kcal/mol, while under $H^+(H_3O^+)$ catalysis it drops to 22.48 kcal/mol. Once the zero point vibrational energy is added, these two values are 29.93 kcal/mol and 24.01 kcal/mol, respectively. It is important to note that, in the case of H^+-catalyzed hydrolysis of disiloxane, the zero point vibrational energy correction increases the activation energy from 22.48 kcal/mol to 24.01 kcal/mol. Part of the reason for the reversal in the correction (compared to water hydrolysis) stems from the structure of the adsorption complex, which is relatively "loose" when compared to the tran-

Table 11 . Hydrolysis Transition State — Activation Energies(Kcal/mol)

	HF/3-21G*	HF/6-31G*	MP2/6-31G*	ΔE^{expt}
$\Delta E_a^{\ddagger 1}$	22.74	44.12	30.43	
$\Delta E_a^{\ddagger 2}$	20.10	40.44	25.62	
$\Delta E_a^{\ddagger 3}$	23.83	42.42	28.17	
$\Delta E_a^{\ddagger 4}$		45.90	31.98	
$\Delta E_a^{\ddagger 5}$	19.71	42.32	28.51	16-21[a]

[1]Based on $H_3SiOH + H_2O^* = H_3SiO^*H + H_2O$
[2]Based on $H_2Si(OH)_2 + H_2O^* = H_2SiOHO^*H + H_2O$
[3]Based on $H_4SiO_4 + H_2O^* = H_4SiO_3O^* + H_2O$
[4]Based on $H_6Si_2O + H_2O^* = H_3SiO^*H + H_3SiOH$
[5]Based on $H_6Si_2O_7 + H_2O^* = H_4SiO_3O^* + H_4SiO_4$
a - Rimstidt and Barnes, 1980; Dove and Crerar, 1990; Dove, 1994

Table 12. Hydrolysis Transition State — $H_6SiOAl + H_2O$ (Kcal/mol)

	HF/3-21G*	HF/6-31G*	MP2/6-31G*	ΔE^{expt}
$\Delta E_a^{\ddagger}$	23.38	35.06	27.23	
ΔE_{ZEC}	-0.62	-0.23	-0.96	
ΔH_o	22.76	34.83	26.27	17-29[a]

a - Helgeson et. al, 1984; Knauss and Wolery, 1986; Rose, 1991

sition state. As we discussed earlier, structures with long bonds tend to have lower frequencies and hence, smaller $\frac{1}{2}h\nu$ corrections. As a result, the zero point vibrational energy is bigger for the transition state than for the stable adsorption complex leading to the increase in the activation barrier.

Analysis of the normal mode associated with the reaction coordinate for the hydrolysis reaction of H_6Si_2O in the presence of $H^+(H_3O^+)$ is shown in Table 15. The motion along the reaction coordinate is quite different from that found for the hydrolysis by H_2O. In the presence of H^+, the motion along the reaction coordinate is dominated by the formation of the new SiO bond and the rupture of the original bridging SiO bond. This is a totally different picture from that in Fig. 13, where the H transfer dominates the hydrolysis reaction. Again, this difference in the character of the motion along the reaction coordinate will manifest itself in major differences in the kinetic isotope effect.

The detailed reaction pathway of such hydrolysis process including the reactant, transition state, and product can be shown in an "ab initio movie" (LASAGA and GIBBS, 1990). One of the commonly used methods to make the movie is to start from the transition state and then go "down hill" along the "steepest decent" direction leading to the reactant and product. Such a calculation will produce the reaction coordinate that forms the basis for the various treatments of transition state theory. Figure 17 is the result of such an effort, which demonstrates the hydrolysis of disiloxane cluster H_6Si_2O under $H^+(H_3O^+)$ catalysis. It shows that once the H_3O^+ approaches the H_6Si_2O, one of the H is transferred to the bridging oxygen site and leads to the formation of a stable adsorption species. The hydrolysis process proceeds with the oxygen of the incoming water forming a new SiO bond with a Si and the original SiO ruptured.

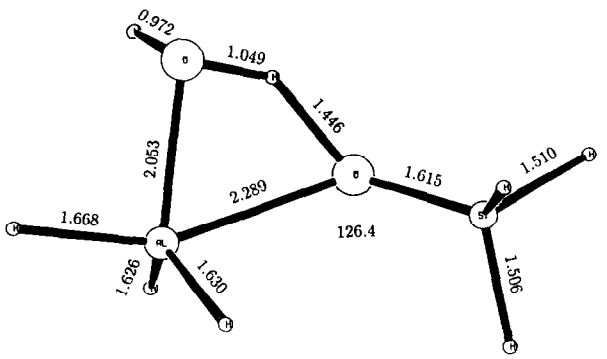

FIG. 15. Fully optimized geometry of the transition state for the hydrolysis reaction of water on a H_6SiOAl group at MP2/6-31G*.

H_3O^+ Hydrolysis of the Si—O—Al Surface Unit

To study the hydrolysis of aluminosilicates in acidic solutions, the activated complex for the hydrolysis of the Si—O—Al moiety needs to be investigated. As already discussed, there is only one adsorption site for H^+ (or H_3O^+) onto Si—O—Al. However, there are two possible activation complexes that can ensue from this adsorption, namely the attachment of the oxygen in the water to either the Si or the Al atoms. Of course, the result is the same, i.e., the hydrolysis of the Si—O—Al structure to produce Si—OH and Al—OH, although in one case, the Si—O bond is broken and in the other case the Al—O bond is broken. Figure 18 shows the fully optimized geometry of the transition state for the case in which the Al—O bond is broken. The calculated $\Delta E_a^{\ddagger}$ and $\Delta H_0^{\ddagger}$ are summarized in Table 16, which shows that the activation energies for either transition state are essentially the same.

The catalytic effect of H^+ adsorption is clear from the data in Tables 12 and 16. The activation energy for the hydrolysis of the Si—O—Al bond in the presence of H^+ is 16.2 kcal/mol, which is significantly lower than the activation energy for uncatalyzed hydrolysis, 27.2 kcal/mol.

Our ab initio studies have focused on the adsorption of H^+ or hydronium ions at the bridging oxygen of Si—O—Si or Si—O—Al units and our studies have also focused on the subsequent hydrolysis reactions at these sites. We believe that reactions on these sites may potentially play an important role in the overall dissolution reaction. As we discussed earlier in this paper, bridging oxygens on silicate surfaces tend to be hydrophobic (ILER, 1979). Therefore, adsorption at these sites is likely very weak. With only a very small proportion of these sites occupied at any time, this type of adsorption may not be directly detectable by surface titration. However, "kinetics does not proceed in a democratic fashion" (LASAGA, 1992). Our ab initio calculations clearly demonstrate that the adsorption of H^+ at the bridging oxygen site significantly

Table 13. Reaction Coordinate normal mode for the $H_6SiOAl - H_2O$ transition state — MP2/6-31G* result (ν = 198.1 i)

Internal Coordinate[a]	Stationary Point[b]	Normal Mode Value[c]
AlO bond	2.289 Å	2.314 Å
AlO bond	2.053 Å	2.041 Å
OH^d bond	1.049 Å	1.103 Å
OH^d bond	1.446 Å	1.353 Å
H^eOH^d angle	108.9°	109.1°
$SiOH^d$ angle	84.4°	81.3°

a - only internal coordinates that involve in reaction are listed
b - see geometry in figure 15
c - value of internal coordinate after vibration is allowed
d - H atom being exchanged in figure 15
e - H atom (unreactive) in water molecule

weakens the Si—O—Al and Si—O—Si linkages and thereby, lowers the energy barrier for reaction by enough kilocalories per mole to overcome the low numbers of such sites present at any one time. Recent work (e.g., BLUM and LASAGA, 1988, 1991), on the other hand, has shown that the dissolution rate of albite and other minerals is directly related to the total amount of adsorbed hydrogen ions on the surface. Our mechanism can only be consistent with this observation if there is a reasonably constant relation between the number of adsorbed hydronium ions on bridging sites and the number of H^+ ions on major adsorption sites such as $SiOH_2^+$, postulating equilibrium in a reaction such as

$$Si - O(H)^+ - Al + Al - OH \rightleftharpoons Si - O - Al + Al - OH_2^+; \quad (12)$$

then, if the number of major free surface sites does not change significantly, such a direct relation would be reasonable.

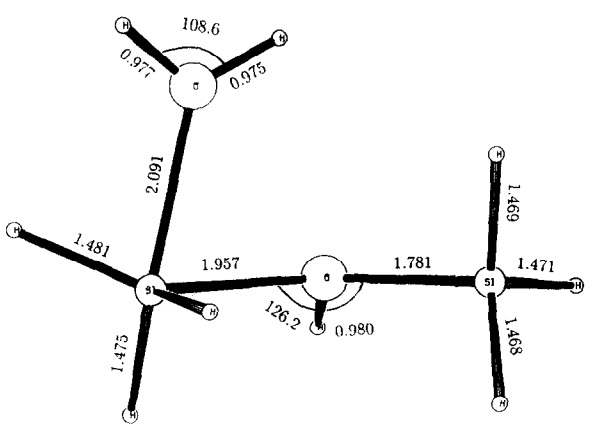

FIG. 16. Fully optimized MP2/6-31G* geometry of the transition state for the hydrolysis of water on a disiloxane group under H^+ catalysis (= disiloxane group hydrolyzed by hydronium H_3O^+).

COMPARISON TO EXPERIMENTAL DATA

Assuming that hydrolysis of the Si—O—Si bond is rate-determining in quartz dissolution, the calculated activation energies should be comparable to those observed in experiments. The activation enthalpies predicted from our activated complexes for the H_2O hydrolysis of H_6Si_2O, as well as other Si—O—Si clusters (namely 26–32 kcal/mol at the MP2 level) are indeed in reasonable agreement with, although several kcal/mol higher than experimental data on the activation energies (16–21 kcal/mol) of quartz dissolution at hydrothermal temperatures (RIMSTIDT and BARNES, 1980; DOVE and CRERAR, 1990). If the mechanism of dissolution involves water adsorption followed by reaction of the water on the surface, then the observed activation energy will include a contribution from the adsorption energy of water (LASAGA, 1981, 1990, 1992), as well as the usual RT term from transition state theory:

$$E_a^{expt} = RT + \Delta H_0^{\ddagger} + \Delta H_{H_2O}^{ads}. \quad (13)$$

$\Delta H_{H_2O}^{ads}$ is expected to be a small negative number (e.g., several kcal/mol). The net effect of the correction in Eqn. 13 would most likely be to lower the calculated E_a by several kcal/mole and so to improve the agreement with experiment.

Note that the activation energy calculated for the H^+ catalyzed hydrolysis of Si—O—Si (24 kcal/mol for the disi-

Table 14. Hydrolysis Transition State — $H_6Si_2O + H_3O^+$ (Kcal/mol)

	HF/3-21G*	HF/6-31G*	MP2/6-31G*	ΔE^{expt}
$\Delta E_a^{\ddagger}$	25.64	25.11	22.48	
ΔE_{ZEC}	1.70	0.90	1.53	
ΔH_o	27.34	26.01	24.01	17-29[a]

a - Helgeson et. al, 1984; Knauss and Wolery, 1986; Rose, 1991

Table 15. Reaction Coordinate normal mode for the H_6Si_2O - H_3O^+ transition state — MP2/6-31G* result (ν = 252.7 i)

Internal Coordinate[a]	Stationary Point[b]	Normal Mode Value[c]
SiO bond	1.957 Å	1.962 Å
SiO bond	2.091 Å	2.082 Å
OH[d] bond	0.980 Å	0.979 Å
OH[e] bond	0.975 Å	0.960 Å
OSiO angle	74.7°	74.8°
SiOH[e] angle	130.7°	129.2°

a - only internal coordinates that involve in reaction are listed
b - see geometry in figure 16
c - value of internal coordinate after vibration is allowed
d - H atom transferred during adsorption, see figure 8
e - H atom (unreactive) in water molecule

loxane cluster) is in better agreement with the observed activation energies. It is still not clear whether H^+ is playing a role in these experiments or not. The overall rate can certainly be written as a sum of the parallel reactions

$$\text{Rate} = X_{H_3O^+,ads}k_{H^+cat} + X_{H_2O,ads}k_{hydrolysis},$$

where $X_{i,ads}$ refers to the concentration of i adsorbed at the reactive surface site and k_i refers to the reaction rate constant

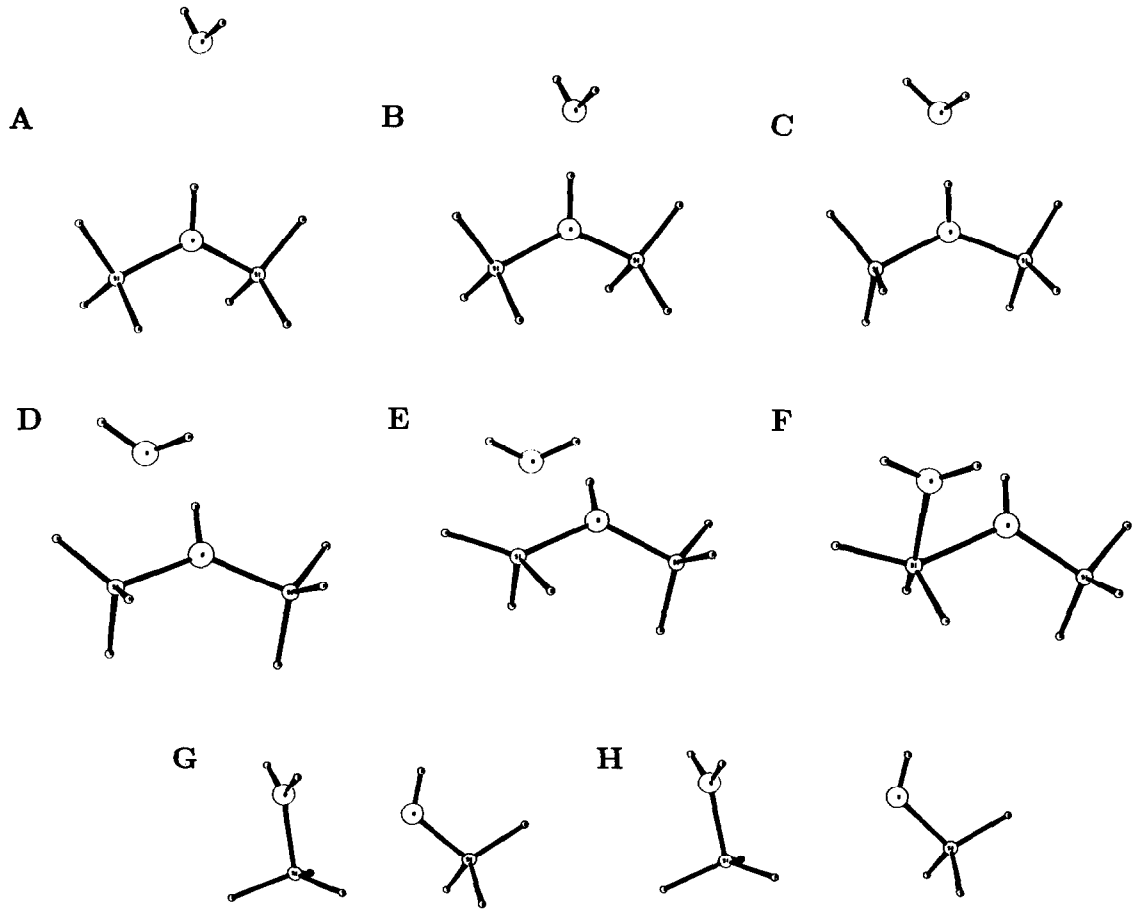

FIG. 17. Ab initio "movie" of the approach, adsorption, and reaction of a water molecule leading to the hydrolysis of the Si—O—Si bond under H^+ catalysis. Calculations used 3-21G* basis set.

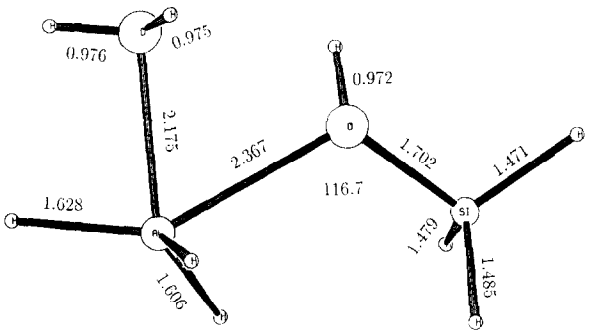

FIG. 18. Fully optimized MP2/6-31G* geometry of the transition state for the hydrolysis of water on a H_6SiOAl group under H^+ catalysis (= H_6SiOAl group hydrolyzed by hydronium H_3O^+).

for the hydrolysis reaction given the particular adsorption site. The two reaction pathways studied in this paper describe each of these two parallel mechanisms. One question that arises, then, is the applicability of the particular ab initio results to the actual reactions being measured. pH is clearly an important parameter in determining the kinetics of mineral reactions. The terms involving the adsorption concentrations are clearly pH dependent. For example, the term $X_{H_3O^+,ads}$ will be relatively high only below the pH_{ZPC} for quartz. On the other hand, the overall rate of the reaction depends not only on the size of the $X_{i,ads}$, but also on the individual rate constants, k_i. If the first term in the last expression refers to the faster reaction, then the calculated activation energy of 24 kcal/mol would be the appropriate one to compare to experiments. However, because there is little dependence of the dissolution rate on pH in the range where many experiments have been performed (excluding the basic solution studies), it would appear that the experimental data are inconsistent with this mechanism, unless the amount of H^+ adsorbed, $X_{H_3O^+,ads}$, was little dependent on the pH. This seems to us to be unlikely, unless the pH is high enough to reach saturation with the surface sites. Thus, the relevant ab initio calculation to compare with the dissolution experiments of quartz in the pH 4–7 range is most likely the water hydrolysis calculation, which yields an activation enthalpy of 29.9 kcal/mol (reduced by the adsorption term as discussed above) from the high level disiloxane calculation. Note, however, the drop in activation energy for the acid catalyzed reaction; we will return to this important point below.

Current studies of the kinetics and mechanisms of aluminosilicate dissolution have focused on the selective hydrolysis of the Si—O—Si or Si—O—Al linkages. Our ab initio calculations predict an energy barrier of 26.3 kcal/mol for the hydrolysis of Si—O—Al by H_2O. The acid catalyzed activation energy is calculated to be 16.0 kcal/mol. Compared to the hydrolysis reactions involving Si—O—Si, there is a much bigger difference between the activation energies of the water hydrolysis and the acid-catalyzed water hydrolysis reactions. Once more, the ab initio results presented here are providing a look at the difference between the acid catalysis of dissolution and the uncatalyzed hydrolysis reaction. It is important to emphasize that both reactions are occurring in parallel in any mineral dissolution (which involves Si—O—Si or Si—O—Al bonds). The relation of these atomic mechanisms to the measured bulk dissolution rate depends on the relative rates of the overall surface reactions.

An obvious experimental quantity to compare with the ab initio results, then, is the measured "activation energy" for feldspar dissolution rates. The dissolution rate of feldspars is certainly pH dependent (e.g., CHOU and WOLLAST, 1985), therefore, the ab initio acid catalyzed activation energy, 16 kcal/mol, is an appropriate figure to use in the comparison. There are some important effects that have to be discussed in carrying out this comparison; but certainly the range of values observed, for example, for the activation energy of the feldspar dissolution (in the acid to neutral pH range) are consistent with our calculations: for albite, 21.2 kcal/mol (HELGESON et al., 1984), 13–29.1 kcal/mol (KNAUSS and WOLERY, 1986), and 17.1 kcal/mol (ROSE, 1991); for sanidine, 12.9 kcal/mol (SCHWEDA, 1989); for microcline, 12.5 kcal/mol (SCHWEDA, 1989).

However, as mentioned, several important factors have to be discussed. One problem that needs to be addressed in comparing the results of the atomic theory discussed here to experiments is the composite nature of the experimental "activation energy," which should be better called the "apparent" activation energy (LASAGA et al., 1994). First, recently there have been a number of papers proposing a pH-dependent activation energy. For example, KNAUSS and WOLERY (1986) obtain E_a = 29 kcal/mol at pH < 3 and E_a = 13 kcal/mol at neutral pH for albite dissolution. Typically, these activation energy changes have produced higher activation energies at low pH than at neutral pH. If one were to simply explain these experimental results as a change in atomic mechanism from acid catalyzed to plain H_2O hydrolysis, that would seem to be inconsistent with the ab initio results, which clearly predict the reverse change in activation energy. This is an important result from this paper. The ab initio results are unlikely to be wrong by such a big difference. Therefore, the reason for the experimentally measured activation energy change with pH has to be looked for elsewhere.

To analyze the experimental temperature dependence of the dissolution rates, all the other factors that can change the rate during these experiments must be studied and understood. In particular, at least two other effects have to be studied. The adsorption of H^+ or H_2O is temperature dependent, as discussed earlier. This temperature dependence will be included in the experimental apparent E_a (e.g., LASAGA et al., 1994). If this temperature dependence itself varied with pH (due to surface charges), then one could obtain a pH-

Table 16. Hydrolysis Transition State — $H_6SiOAl + H_3O^+$ (Kcal/mol)

	HF/3-21G*	HF/6-31G*	MP2/6-31G*	ΔE^{expt}
$\Delta E_a^{\ddagger}$	20.03(20.28)	16.53(16.65)	16.18(16.23)	
ΔE_{ZEC}	-0.04(-0.12)	-0.26(-0.25)	-0.31(-0.28)	
ΔH_o	19.99(20.16)	16.27(16.40)	15.87(15.95)	17-29[a]

* - numbers in ( ) are based on $H_6AlOSi + H_3O^+$

a - Helgeson et. al, 1984; Knauss and Wolery, 1986; Rose, 1991

dependent apparent activation energy (CASEY and SPOSITO, 1992). In this case, the temperature dependence of the adsorption would have to be measured first and subtracted out to obtain the relevant activation energy to compare with atomic theories (e.g., LASAGA et al., 1994). A second complication can arise because many studies have not corrected for an important effect arising from variations in ΔG during the experiments. Thus, if the pH is fixed and the temperature is varied, the ΔG of the reaction is not constant, even for similar solution compositions. This effect is not important if the ΔG is sufficiently negative (far from equilibrium), but the ΔG values would have to be less than -9 kcal/mol for the case of albite (BURCH et al., 1993). Under these restrictions, many experiments may not be in the far-from-equilibrium region (e.g., see BURCH et al., 1993).

Both the adsorption effects and the effects of varying ΔG can have significant effects on the magnitude and variation of the apparent activation energy. These effects must be eliminated if a truly atomic activation energy is to be extracted from the experiments. The ab initio results not only are providing a reverse trend in the activation energy with pH, but they are also strongly indicating that the other effects, such as mentioned above, are having a sizeable influence on the rates being measured (and hence, on the "apparent" activation energies). This prediction from the ab initio results will have to be checked out in future experiments and theoretical studies.

Another important result from the ab initio calculations is that the calculated activation enthalpy for the acid hydrolysis of H_6SiOAl, 16.2 kcal/mol, is more than 6 kcal/mol less than the calculated activation energy for the acid hydrolysis of H_6Si_2O, 22.5 kcal/mol. Such a difference in activation energy would predict that it would be easier to hydrolyze Si—O—Al linkages than Si—O—Si linkages in silicate dissolution. Such preferential hydrolyzation of Si—O—Al has been previously discussed in the literature (e.g., BRADY and WALTHER, 1989; BLUM and LASAGA, 1991). So the ab initio results, in this case, provide atomic evidence for these proposed hypotheses. Preferential hydrolyzation of Si—O—Al would lead to the preferential release of Al from the surface and, thereby, form a leached layer rich in silica under acidic conditions. Such leached layers have, in fact, been observed in kinetic experiments involving dissolution of feldspars under low pH conditions. For example, many recent studies of the kinetics of albite dissolution, using a variety of spectroscopic techniques, have shown that leached zones depleted in Na, Al, and O formed during the initial, incongruent phase of dissolution. This zone may extend as deep as 1000 Å or more at pH values of 1 or 2 (CASEY et al., 1988, 1989a,b; HELLMANN et al., 1990).

Kinetic Isotope Effect and the Mechanisms of Silicate Dissolution

Useful structural and dynamic information on the reaction mechanism can usually be obtained from the kinetic isotope effect (MELANDER and SAUNDERS, 1980). This is because the kinetic isotope effect is directly related to the mass dependence of the reaction coordinate. The mass dependence will be significant for reactions in which atoms are involved in bond-forming and bond-breaking processes along the reaction coordinate (Primary Isotope Effect). As a result, the combined theoretical and experimental studies of isotope effects in mineral surface chemistry can open a unique window to the specific transition state structure and the elementary reaction controlling a surface reaction.

Based on the calculated reaction potential surfaces, the kinetic isotope effects can be calculated using various statistical and collision kinetic theories. At the level of the harmonic approximation, the standard statistical mechanical expressions for the translational, rotational, and vibrational partition functions can be used to evaluate the transition state rate constant. The kinetic isotope effect for a reaction involving hydrolysis after adsorption is given by VAN HOOK (1970):

$$\frac{k^*}{k} = \frac{\nu^{\ddagger *}}{\nu^{\ddagger}} \frac{\Gamma^{\ddagger *}_{\text{tunn}}}{\Gamma^{\ddagger}_{\text{tunn}}} \frac{\prod_i \frac{h\nu_i^{\ddagger *}}{kT}(1 - \exp(-h\nu_i^{\ddagger}/kT))}{\prod_i \frac{h\nu_i^{\ddagger}}{kT}(1 - \exp(-h\nu_i^{\ddagger *}/kT))} \cdot \frac{\prod_i \frac{h\nu_i^{\text{ads}}}{kT}(1 - \exp(-h\nu_i^{\text{ads}*}/kT))}{\prod_i \frac{h\nu_i^{\text{ads}*}}{kT}(1 - \exp(-h\nu_i^{\text{ads}}/kT))} e^{-(\Delta E^{\ddagger *} - \Delta E^{\ddagger}/RT)}, \quad (14)$$

where ν_i^{ads} and $\nu_i^{\text{ads}*}$ refer to the vibrational frequencies of the two isotopic variants of the adsorbed molecule that is reacting; $\nu_i^{\ddagger}$ and $\nu_i^{\ddagger *}$ refer to the normal frequencies of the isotopic variants of the activated complex for the surface reaction. $\nu^{\ddagger}$ and $\nu^{\ddagger *}$ refer to the single imaginary frequencies of the corresponding activated complexes. The difference in activation energies in the exponent is obtained from

$$\Delta E^{\ddagger *} - \Delta E^{\ddagger} = \sum_i \frac{1}{2} h\nu_i^{\ddagger *} - \sum_i \frac{1}{2} h\nu_i^{\ddagger} - \sum_i \frac{1}{2} h\nu_i^{\text{ads}*} + \sum_i \frac{1}{2} h\nu_i^{\text{ads}}. \quad (15)$$

The tunneling correction ($\Gamma^{\ddagger}_{\text{tunn}}$) arises from quantum mechanical tunneling through the activation barrier along the reaction coordinate. Tunneling is generally important only for primary isotope effects in reactions involving H transfer. Therefore, in considering the hydrogen-deuterium isotope effect for the hydrolysis of H_6Si_2O by H_2O, the correction would be nontrivial. A simple calculation would use the first order Wigner approximation:

$$\Gamma^{\ddagger}_{\text{tunn}} = 1 + \frac{1}{24}\left(\frac{h\nu^{\ddagger}}{kT}\right)^2, \quad (16)$$

where $\nu^{\ddagger}$ is the absolute value of the reaction coordinate imaginary frequency from ab initio calculations. For detailed calculation of the tunneling correction, kineticists generally use the transmission coefficients from the Eckart barrier (e.g., JOHNSTON, 1966). An even higher calculation will use the variational transition state theory (VTST) (KREEVOY and TRUHLAR, 1986), which requires a thorough investigation of the curvature of the potential along the entire reaction coordinate. However, at or above room temperature, the difference between those tunneling corrections becomes small

(TRUONG and TRUHLAR, 1990) and the Wigner method should give a reasonable correction.

LASAGA and GIBBS (1990) and CASEY et al. (1990) applied Eqn. 14 to the hydrolysis reaction of silica using H_3SiOH and the higher cluster H_6Si_2O, respectively. By replacing the incoming H_2O with D_2O, they predicted that the dissolution rate of quartz in H_2O should be faster than that in D_2O by a factor of 3 to 4. Results from our newest calculations based on H_6Si_2O hydrolysis at the MP2/6-31G* level are listed in Table 17, and are in good agreement with their ab initio results.

The reason for the large kinetic isotope effect in this case is that hydrogen transfer is the dominant change along the reaction coordinate. Table 17 shows that the biggest contribution to the calculated kinetic isotope effect is from the difference in activation energies (the last term of Eqn. 14), which indicates that the energy barrier difference between quartz dissolution in D_2O and in H_2O is nontrivial. This difference arises solely from changes in the vibrational frequencies (Eqn. 15). Because D_2O has heavier masses, the frequencies will be lower (recall $\nu = (1/2\pi)\sqrt{k/m}$ in simple vibrations) and decrease the zero-point vibrational energy correction. Our calculation shows that the activation energy for quartz dissolution in D_2O should be 1.3 kcal/mol higher than that in H_2O.

Table 17 also lists the experimental values for quartz dissolution in H_2O and D_2O at pH 3 and 25–70°C from CASEY et al. (1990). The experiments were designed to test their proposed mechanism of silica dissolution, i.e., the hydrolysis of the Si—O—Si bond by H_2O. The reason they chose pH 3 is that the pH of zero point charge of quartz, pH_{zpc}, is 2.4 at 25°C (PARKS, 1967), and the quartz dissolution rate is nearly independent of solution pH at $2 < pH < 4$ (e.g., HIEMSTRA and VAN RIEMSDIJK, 1990). Under this condition, it is generally believed that the dissolution reaction may involve only hydrolysis by water (e.g., KNAUSS and WOLERY, 1988; DOVE and CRERAR, 1990; LASAGA and GIBBS, 1990; DOVE, 1994) with no net enhancement by adsorbed hydrogen or hydroxyl ions. The experimental average for the ratio of the rate constants, $k_{H_2O}/k_{D_2O} = 1.17\ (\pm 0.17)$, is significantly different from the ab initio result of 3–4. In addition, the measured activation energy at this temperature range (8.7 kcal/mol) is much lower than those from hydrothermal experiments (16–21 kcal/mol), as well as from ab initio calculations. The data in CASEY et al. (1990) is still controversial and thus, it may be that the disagreement stems from experimental difficulties. On the other hand, an alternative explanation is that the hydrogen transfer from water to the bridging oxygen under the experimental conditions is more rapid than modeled and may proceed early in the overall reaction (CASEY et al., 1990). The discrepancy may also be attributed to a mechanism change from hydrothermal temperatures to diagenetic and weathering temperatures (LASAGA, 1992), however, more experimental isotopic data are needed (e.g., at hydrothermal temperatures) to verify this point and to ascertain the predictions of the ab initio calculations.

Table 17. Kinetic isotope effect on quartz dissolution - *ab initio* vs experiment

Temperature(°C)	20	30	40	50	60	70
Vib ratio	1.38	1.38	1.38	1.39	1.39	1.39
E_a ratio	3.14	3.02	2.92	2.82	2.73	2.65
Tunneling	1.30	1.29	1.28	1.26	1.25	1.24
k_{H_2O}/k_{D_2O} [a]	5.81	5.56	5.32	5.13	4.93	4.74
Vib ratio	1.09	1.09	1.08	1.08	1.08	1.07
E_a ratio	0.70	0.71	0.71	1.72	1.73	1.73
Tunneling	1.00	1.00	1.00	1.00	1.00	1.00
$k_{H_3O^+}/k_{D_3O^+}$ [b]	0.76	0.76	0.77	0.77	0.78	0.78
Experiment[c]	1.26	1.00	1.16	1.14	1.28	1.25

a - Based on $H_6Si_2O + H_2O = H_3SiOH + H_3SiOH$
b - Based on $H_6Si_2O + H_3O^+ = H_3SiOH_2^+ + H_3SiOH$
c - Casey et. al., 1990

The acid-catalyzed hydrolysis of Si—O—Si shows quite different isotope effects. Recall the fact that the hydrolysis of the Si—O—Si bond under $H^+(H_3O^+)$ catalysis has a much lower activation energy than the uncatalyzed water hydrolysis (24 kcal/mol vs. 29.9 kcal/mol). Analyzing the trajectory of the reaction along the reaction coordinate, the H is transferred to the bridging oxygen early in the H_3O^+ adsorption stage for the case of acid-catalyzed hydrolysis. The normal mode analysis of the reaction coordinate in the vicinity of the transition state shows that none of the hydrogen atoms are active. These results suggest that there should be a small, secondary isotope effect for the hydrolysis reaction involving H_3O^+. Indeed, the calculated isotope effect based on this new model gives a small kinetic isotope effect (Table 17), i.e., $k_{H_3O^+}/k_{D_3O^+} = 0.77$, which is closer to the experimental value than that based on the uncatalyzed water hydrolysis of Si—O—Si.

Interestingly, our new calculation predicts that $k_{H_3O^+}/k_{D_3O^+} < 1$, suggesting that the quartz dissolution should be faster in heavy water than in normal water if the hydrolysis is catalyzed by $H^+(H_3O^+)$. This phenomenon (reversed isotope effect) has usually been related to the so-called "kinetic steric isotope effects" (MELANDER and SAUNDERS, 1980). If the reaction is limited by space considerations (i.e., it is sterically hindered), the rate is expected to be more rapid in D_2O than in H_2O because protium "requires more space" than deuterium (CARTER and MELANDER, 1973). As a matter of fact, GRATZ and BIRD (1993a,b) reported that quartz dissolution in D_2O is about 35% faster than in H_2O. However, because their experiment was carried out in 0.01 M KOH solutions, the dissolution process most likely involved OH catalysis. In our case, this "unusual" kinetic isotope effect stems from two factors: (1) The structure of the adsorption complex is relatively "loose," compared to the transition state. As a result, the zero point energy correction raises (opposite to the usual case) the energy barrier from 22.5 kcal/mol to 24.0 kcal/mol. (2) The substitution of H_3O^+ by D_3O^+ lowers the vibrational frequencies and thus, decreases the zero-point energy correction. The smaller zero-point energy correction for the D_3O^+-catalyzed hydrolysis reaction will lead to a lower activation energy and thus cause faster quartz dissolution in D_3O^+ than in H_3O^+. Our calculation suggests that the activation energy for quartz dissolution in D_3O^+ should be 0.4 kcal/mol lower than in H_3O^+. Future experiments, as well

as theoretical investigations are needed to verify the "unusual" kinetic isotope effects at both low and high pH.

It is important to point out that for any complex reaction such as quartz dissolution, the observed kinetic isotope effect is a weighted average of isotope effects from all elementary steps which control the overall rate. The comparison between the ab initio and experimental results suggests that both "pure water" hydrolysis and H^+ catalyzed hydrolysis are the elementary reactions controlling the overall quartz dissolution at low pH, with H^+ catalysis being the dominant one. However, the dissolution rate is not pH dependent and so the acid catalysis mechanism (which also gave better agreement between ab initio and experimental activation energies) was not favored earlier in this paper. It is clear that closer scrutiny of the kinetic isotope effect may enable us to pinpoint further which atomic processes are dominating the dissolution reaction of quartz.

We also calculated the kinetic isotope effects for the hydrolysis of the Si—O—Al bond. Table 18 gives the ab initio results based on the water hydrolysis model (no catalysis). Our calculations only yield a factor of 1.66, i.e., the dissolution rate of aluminosilicates such as feldspar in H_2O should only be 70% times faster than in D_2O, if the hydrolysis of Si—O—Al bonds controls the overall dissolution rate. This isotope effect is much smaller than that obtained for the hydrolysis of Si—O—Si groups by H_2O. The reason for the difference is that the hydrogen transfer occurs later in the hydrolysis of the Si—O—Al bond. Thus, the transition state structures for the H_2O hydrolysis of Si—O—Si and Si—O—Al have the hydrogen, that is being transferred, at quite different positions. For the Si—O—Si hydrolysis transition state, the OH distances (Fig. 13) are quite similar (1.230 Å vs. 1.187 Å), and so the hydrogen transfer is active in the region around the transition state. In the Si—O—Al hydrolysis transition state (Fig. 15), the two OH distances are quite different (1.049 Å vs. 1.446 Å), so that the hydrogen is transferred at a later stage in the hydrolysis reaction (i.e., after the transition state has been crossed). This difference has also been reflected by the calculated vibrational frequencies of the transition states as well as the tunneling corrections.

Table 18. Kinetic isotope effect on feldspar dissolution - *ab initio*

Temperature(°C)	20	30	40	50	60	70
Vib ratio	1.19	1.19	1.19	1.19	1.19	1.19
E_a ratio	1.46	1.44	1.42	1.41	1.39	1.38
Tunneling	1.00	1.00	1.00	1.00	1.00	1.00
k_{H_2O}/k_{D_2O}[a]	1.72	1.70	1.68	1.67	1.65	1.64
Vib ratio	1.01	1.01	1.01	1.00	1.00	1.00
E_a ratio	1.08	1.06	1.07	1.07	1.07	1.07
Tunneling	1.00	1.00	1.00	1.00	1.00	1.00
$k_{H_3O^+}/k_{D_3O^+}$[b]	1.08	1.08	1.08	1.07	1.07	1.06
Experiment[c]	1.49	1.49	1.49	1.49	1.49	1.49

a - Based on $H_6SiOAl + H_2O = H_3AlOH + H_3SiOH$
b - Based on $H_6SiOAl + H_3O^+ = H_3AlOH_2^+ + H_3SiOH$
c - feldspar dissolution at pH 1-2 (Casey et. al., 1988)

Based on the transition state for the hydrolysis of H_6Si_2O by water, the imaginary frequency is 1084 i cm^{-1}. However, the imaginary frequency from the transition state for the hydrolysis of H_6SiOAl by water is much lower at 198.1 i cm^{-1}. Since the dominant normal mode in the case of Si—O—Al hydrolysis is largely the formation of a new AlO bond and the rupture of an original AlO bond, all involving atoms with heavy masses, the tunneling effect is expected to be small.

There are several sets of experimental data on the kinetic isotope effects in silicate glass as well as feldspar dissolution. For example, CASEY et al. (1988) found that the dissolution rates of labradorite feldspar in H_2O—HCl solutions (pH = 1.7) are 50% more rapid than in D_2O—DCl mixtures (pD = 1.7) (k_{H_2O}/k_{D_2O} = 1.49). These experiments at low pH can be compared to the H^+(H_3O^+) catalyzed model for the hydrolysis of Si—O—Al. The calculated results are summarized in Table 18. It shows that the hydrolysis rate in the H^+—H_2O system is only slightly faster than in the D^+—D_2O system ($k_{H_3O^+}/k_{D_3O^+}$ = 1.07). Again, we find a discrepancy between theory and experiment. It is interesting that, this time, the ab initio kinetic isotope effect based on pure water hydrolysis is quite close to the experimental one for feldspar. It is clear that, while the isotope effects have the potential to unravel details of the reaction mechanism, both the theoretical work and the experimental studies need some further refinement.

Currently, similar calculations are being carried out to study the kinetics and mechanisms of silicate dissolution under OH^- catalysis. Another set of investigation is underway to explore the effects of adsorbed cations on water-rock surface reactions. Recent experiments (DOVE and CRERAR, 1990; DOVE, 1994) have shown that hydrothermal dissolution of quartz can be significantly catalyzed by Na^+ and K^+ in the solution. The explanation of the catalytic effect should be related to the adsorption of those cations on quartz surface.

CONCLUSIONS

The need for a fundamental atomic theory of the chemical processes occurring at mineral surfaces has become increasingly important. For the first time, ab initio methods are providing key information on the details of relevant atomic dynamics leading to important reactions such as adsorption, acid-base catalysis, dissolution, and precipitation. In our study, the surface energetics and the bonds governing adsorption and chemical reactions are all obtained from calculations on molecular clusters of various sizes. Results so far indicate that the assumption that the bond-making and bond-breaking processes in many geochemical reactions such as silicate dissolution processes are mostly short-range in nature is a rather good assumption. Therefore, the dynamics of many of these reactions is controlled by a small set of atoms and long-range effects involving many unit cells are minimal.

Using such finite molecular clusters, this paper has discussed the detailed molecular mechanism for the adsorption of both water and acid species (e.g., H^+ and H_3O^+) onto silica and aluminosilicate surfaces. In addition, the paper has discussed the reaction pathway for the breaking of Si—O—Si and Si—O—Al structural units on the surfaces

of minerals. The catalytic effect of acids in promoting the dissolution process has been specifically addressed here. Finally, the actual molecular trajectories involved in the entire dissolution process on mineral surfaces (e.g., adsorption, the ensuing formation of the transition state and the breakdown of the activated complex to form products) have been obtained to produce a first principles ab initio "movie" of the dissolution.

Our major conclusions include:

1) The kinetics of quartz and feldspar dissolution at low pH involves two mechanisms, i.e., H_2O hydrolysis and $H^+(H_3O^+)$ catalysis.
2) There is only one unique adsorption site for both water and the hydronium ion onto the Si—O—Al surface unit. Thus, the adsorption occurs at distances roughly equal to both the Si and Al atoms of the bridging unit.
3) The adsorption of $H^+(H_3O^+)$ onto the bridging oxygen sites of Si—O—Si and Si—O—Al linkages plays the key role in catalyzing the dissolution process. Calculated activation energies agree well with experimental data.
4) The $H^+(H_3O^+)$ catalysis reaction pathway leads to major changes in the potential surface and the reaction coordinate. These changes lead to not only lower activation energies, but also to smaller kinetic isotope effects, much closer to experimental data at low temperatures.
5) The activation energies for the H^+-catalyzed reactions have been found to be distinctly lower than those for water hydrolysis, $E_a(H_3O^+) < E_a(H_2O)$. This result is in the opposite direction to the pH-dependent "apparent" experimental activation energies. The ab initio results show that the effects of other factors (e.g., adsorption or ΔG factors) are quite significant in the overall activation energies obtained for feldspar dissolution.
6) The acid-catalyzed hydrolysis of the Si—O—Al bond is calculated to be preferred over the acid-catalyzed hydrolysis of the Si—O—Si bond, which explains, using first principles, the observed formation of leached layers at low pH in feldspar dissolution studies.
7) There still remain big inconsistencies between the experimental and the theoretical kinetic isotope effects, both for quartz and feldspar dissolution. Because the isotope effects are sensitive to the reaction path, this discrepancy is important and needs to be studied further in the future.

Acknowledgments—The author would like to gratefully acknowledge financial support from the National Science Foundation (NSF EAR 9017976 and 9219770) and the funding through the Branch of Energy Science of the Department of Energy (grant DE-FG02-90-ER14153). The authors would also like to thank the thorough reviews by Patrick Brady, Patricia Dove, and an anonymous reviewer.

Editorial handling: M. F. Hochella Jr.

REFERENCES

AAGAARD P. and HELGESON H. C. (1982) Thermodynamic and kinetic constraints on reaction rates among minerals and aqueous solutions, I. Theoretical considerations. *Amer. J. Sci.* **282**, 237–235.

ANGELL C. A., SCAMEHORN C. A., PHIFER C. C., KADIYALA R. R., and CHEESEMAN P. A. (1988) Ion dynamics studies of liquid and glassy silicates, and gas-liquid solutions. *Phys. Chem. Mineral* **15**, 221–227.

BARROW M. J., EBSWORTH E. A. V., and HARDING M. M. (1979) The crystal and molecular structures of disiloxane (at 108k) and hexamethyldisiloxane (at 148 K). *Acta Crystall.* **B35**, 2093–2099.

BENNETT P. C. (1991) Quartz dissolution in organic-rich aqueous systems. *Geochim. Cosmochim. Acta* **55**, 1781–1797.

BLUM A. E. and LASAGA A. C. (1988) Role of surface speciation in the low-temperature dissolution of minerals. *Nature* **331**, 431–433.

BLUM A. E. and LASAGA A. C. (1991) The role of surface speciation in the dissolution of albite. *Geochim. Cosmochim. Acta* **55**, 2193–2201.

BRADY P. V. (1992) Silica surface chemistry at elevated temperatures. *Geochim. Cosmochim. Acta* **56**, 2941–2946.

BRADY P. V. and WALTHER J. V. (1989) Controls on silicate dissolution rates in neutral and basic pH solutions at 25°C. *Geochim. Cosmochim. Acta* **53**, 2823–2830.

BRADY P. V. and WALTHER J. V. (1990) Kinetics of quartz dissolution at low temperatures. *Chem. Geol.* **82**, 253–264.

BURCH T. E., NAGY K. L., and LASAGA A. C. (1993) Free energy dependence of albite dissolution kinetics at 80°C and pH 8.8. *Chem. Geol.* **105**, 137–162.

BURKHARD D. J. M., DE JONG B. H. W. S., MEYER A. J. H. M., and VAN LENTHE J. H. (1991) $H_6Si_2O_7$: Ab initio molecular orbital calculations show two geometric conformations. *Geochim. Cosmochim. Acta* **55**, 3453–3458.

CAROLL-WEBB S. A. and WALTHER J. V. (1988) A surface complex reaction model for the pH-dependence of corundum and kaolinite dissolution rates. *Geochim. Cosmochim. Acta* **52**, 2609–2623.

CARTER R. E. and MELANDER L. (1973) Experiments on the nature of steric isotope effects. *Advances Phys. Org. Chem.* **182**, 141–156.

CASEY W. H. and SPOSITO G. (1992) On the temperature dependence of mineral dissolution rates. *Geochim. Cosmochim. Acta* **56**, 3825–3830.

CASEY W. H., WESTRICH H. R., and ARNOLD G. W. (1988) Surface chemistry of labradorite feldspar reacted with aqueous solutions at pH = 2, 3, and 12. *Geochim. Cosmochim. Acta* **52**, 2795–2807.

CASEY W. H., WESTRICH H. R., ARNOLD G. W., and BANFIELD J. F. (1989a) The surface chemistry of dissolving labradorite feldspar. *Geochim. Cosmochim. Acta* **53**, 821–832.

CASEY W. H., WESTRICH H. R., ARNOLD G. W., and BANFIELD J. F. (1989b) The surface of labradorite feldspar after acid hydrolysis. *Chem. Geol.* **78**, 205–218.

CASEY W. H., LASAGA A. C., and GIBBS G. V. (1990) Mechanisms of silica dissolution as inferred from the kinetic isotope effect. *Geochim. Cosmochim. Acta* **54**, 3369–3378.

CHAKONMAKOS B. C. and GIBBS G. V. (1986) Theoretical molecular orbital study of silanol-water interactions. *J. Phys. Chem.* **90**, 996–998.

CHOU L. and WOLLAST R. (1984) Study of the weathering of albite at room temperature and pressure in a fluidized bed reactor. *Geochim. Cosmochim. Acta* **48**, 2205–2118.

CHOU L. and WOLLAST R. (1985) Steady-state kinetics and dissolution mechanisms of albite. *Amer. J. Sci.* **285**, 963–993.

DAMRAUER R., BURGGRAF L. W., DAVIS L. P., and GORDON M. S. (1988) Gas-phase and computational studies of pentacoordinate silicon. *J. Amer. Chem. Soc.* **110**, 6601–6606.

DAVIS J. A. and LECKIE J. O. (1979) Speciation of adsorbed ions at the oxide/water interface. In *Chemical Modeling in Aqueous Systems* (ed. JENNE E. A.): *Amer. Chem. Soc. Symp. Ser. 93*, pp. 299–320.

DEJONG B. H. W. S. and BROWN G. E., JR. (1980) Polymerization of silicate and aluminate tetrahedra in glasses and melts and aqueous—II. The network modifying effects of Mg^{2+}, K^+, Na^+, Li^+, H^+, OH^-, F^-, Cl^-, H_2O, CO_2, and H_3O^+ on silicate polymers. *Geochim. Cosmochim. Acta* **44**, 1627–1642.

DIBBLE W. E., JR. and TILLER W. A. (1981) Non-equilibrium water-rock interactions—I model for interface-controlled reactions. *Geochim. Cosmochim. Acta* **45**, 79–92.

DOVE P. M. (1994) The dissolution kinetics of quartz in sodium chloride solutions at 25°C to 300°C. *Amer. J. Sci.* **294**, 665–712.

DOVE P. M. and CRERAR C. A. (1990) Kinetics of quartz dissolution

in electrolyte solutions using a hydrothermal mixed flow reactor. *Geochim. Cosmochim. Acta* **54,** 955–969.

DOVE P. M. and ELSTON S. F. (1992) The low-temperature dissolution kinetics of quartz in sodium chloride solutions: Analysis of existing data and a rate model for 25°C, pH 2–13. *Geochim. Cosmochim. Acta* **56,** 4147–4156.

DOVESI R., PISANI C., and SILVI B. (1987) The electronic structure of α-quartz: A periodic Hartree-Fock calculation. *J. Chem. Phys.* **86,** 6967–6971.

FRISCH M. J. et al. (1990) *"Gaussian 90."* Gaussian, Inc.

FRISCH M. J. et al. (1992) *"Gaussian 92."* Gaussian, Inc.

FURRER G. and STUMM W. (1986) The coordination chemistry of weathering: I Dissolution kinetics of α-Al_2O_3 and BeO. *Geochim. Cosmochim. Acta* **50,** 1847–1860.

GARRONE E. and UGLIENGO P. (1989) Silanol as a model for the free hydroxyl of amorphous silica: Non-empirical calculations of the vibrational features of H_3SiOH. In *Structure and Reactivity of Surfaces* (ed. C. MORTERRA et al.), pp. 405–412. Elsevier.

GEERLINGS P., TARIEL N., BOTREL A., LISSILLOUR R., and MORTIER W. J. (1984) Interaction of surface hydroxyls with adsorbed molecules. A quantum chemical study. *J. Phys. Chem.* **88,** 5752–5759.

GEISINGER K. L. and GIBBS G. V. (1981) STO-3G molecular orbital (MO) calculated correlations of tetrahedral SiO and AlO bridging bond lengths with p_0 and f_s. *GSA Abstr. Prog.* **13,** 458 (abstr.).

GIBBS G. V. (1982) Molecules as models for bonding in silicates. *Amer. Mineral.* **67,** 421–450.

GRATZ J. G. and BIRD P. (1993a) Quartz dissolution: negative crystal experiments and a rate law. *Geochim. Cosmochim. Acta* **57,** 965–976.

GRATZ J. G. and BIRD P. (1993b) Quartz dissolution: theory of rough and smooth surfaces. *Geochim. Cosmochim. Acta* **57,** 977–989.

HEHRE W. J., RADOM L., SCHLEYER P. R., and POPLE J. A. (1986) *Ab initio Molecular Orbital Theory.* Wiley.

HELGESON H. C., MURPHY W. M., and AAGAARD P. (1984) Thermodynamic and kinetic constraints on reaction rates among minerals and aqueous solutions. II. Rate constants, effective surface area, and the hydrolysis of feldspar. *Geochim. Cosmochim. Acta* **48,** 2405–2432.

HELLMANN R. (1994) The albite-water system. Part I: The kinetics of dissolution as a function of pH at 100, 200 and 300°C. *Geochim. Cosmochim. Acta* **58,** 595–612.

HELLMANN R., EGGLESTON C. M., HOCHELLA M. F., JR., and CRERAR D. A. (1990) The formation of leached layers on albite surfaces during dissolution under hydrothermal conditions. *Geochim. Cosmochim. Acta* **54,** 1267–1281.

HIEMSTRA T. and VAN RIEMSDIJK W. H. (1990) Multi activated-complex dissolution of metal(hydr)oxides: A thermodynamic treatment. *J. Colloid Interface Sci.* **136,** 132–150.

HIEMSTRA T., VAN RIEMSDIJK W. H., and BOLT G. H. (1989a) Multisite proton adsorption modeling at the solid/solution interface of (hydo)oxides: a new approach I. Model description and evaluation of intrinsic reaction constants. *J. Colloid Interface Sci.* **133,** 91–104.

HIEMSTRA T., DE WIT J. C. M., and VAN RIMSDIJK W. H. (1989b) Multisite proton adsorption modeling at the solid/solution interface of (hydo)oxides: A new approach II. Application to various important (hydr)oxides. *J. Colloid Interface Sci.* **133,** 105–117.

HOBZA P., SAUER J., MOREGENYER C., HURYCH J., and ZAHRADNIK R. (1981) Bonding ability of surface sites on silica and their effect on hydrogen bonds. A quantum-chemical and statistical thermodynamic treatment. *J. Phys. Chem.* **85,** 4061–4067.

ILER N. (1979) *The Chemistry of Silica.* Wiley.

JOHNSTON H. S. (1966) *Gas Phase Reaction Rate Theory.* Ronald Press.

KNAUSS K. G. and WOLERY T. J. (1986) Dependence of albite dissolution kinetics on pH and time at 70°C. *Geochim. Cosmochim. Acta* **50,** 2481–2498.

KNAUSS K. G. and WOLERY T. J. (1988) The dissolution kinetics of quartz as a function of pH and time at 70°C. *Geochim. Cosmochim. Acta* **52,** 43–53.

KREEVOY M. M. and TRUHLAR D. G. (1986) Transition State Theory. In *Investigation of Rates and Mechanisms of Reactions* (ed. C. F. BERNASCONI); *Techniques of Chemistry,* Vol. VI, pp. 13–95. Wiley-Interscience.

KUBICKI J. D. and LASAGA A. C. (1990) Molecular dynamics and diffusion in silicate melts. In *Diffusion, Atomic Ordering, and Mass Transport* (ed. J. GANGULY); *Advances in Physical Geochem. 8,* pp. 1–50.

KUBICKI J. D., XIAO Y., and LASAGA A. C. (1993) A theoretical reaction path for the $^{[4]}Si \rightarrow {}^{[5]}Si$ coordination change and deprotonation of orthosilicic acid in basic solution. *Geochim. Cosmochim. Acta* **57,** 3847–3853.

LASAGA A. C. (1981) Transition state theory. In *Kinetics of Geochemical Processes* (ed. A. C. LASAGA and R. J. KIRKPATRICK); *Rev. Mineral. 8,* pp. 135–169.

LASAGA A. C. (1984) Chemical kinetics of water-rock interactions. *J. Geophys. Res.* **B6,** 4009–4025.

LASAGA A. C. (1990) Atomic treatment of mineral-water surface reactions. In *Mineral-Water Interface Geochemistry* (ed. M. F. HOCHELLA, JR. and A. F. WHITE); *Rev. Mineral. 23,* pp. 17–80.

LASAGA A. C. (1992) Ab initio methods in mineral surface reactions. *Rev. Geophys.* **30/3,** 269–303.

LASAGA A. C. and GIBBS G. V. (1987) Application of quantum mechanical potential surfaces to mineral physics calculation. *Phys. Chem. Mineral.* **14,** 107–117.

LASAGA A. C. and GIBBS G. V. (1988) Quantum mechanical surfaces and calculations on minerals and molecular clusters. *Phys. Chem. Mineral.* **16,** 29–41.

LASAGA A. C. and GIBBS G. V. (1989) Ab initio quantum mechanical calculations of surface reactions—A new era? In *Aquatic Chemical Kinetics* (ed. W. STUMM), pp. 259–289. Wiley.

LASAGA A. C. and GIBBS G. V. (1990) Ab initio quantum mechanical calculations of water-rock interactions: Adsorption and hydrolysis reactions. *Amer. J. Science* **290,** 263–295.

LASAGA A. C. and GIBBS G. V. (1991) Quantum mechanical Hartree-Fock surfaces and calculations on minerals. II. 6-31G* results. *Phys. Chem. Mineral.* **17,** 485–491.

LASAGA A. C., SOLER J. M., GANOR J., BURCH T. E., and NAGY K. L. (1994) Chemical weathering rate laws and global geochemical cycles. *Geochim. Cosmochim. Acta* **58,** 2361–2386.

MARTIN J. L., FRANCOIS J. P., and GIJBELS R. (1989) Combined bond-polarization basis sets for accurate determination of dissolution energies. II: Basis set superposition error as a function of the parent basis set. *J. Comput. Chem.* **10,** 875–886.

MCMILLAN P. F. and KIRKPATRICK R. J. (1992) Al coordination in magnesium aluminosilicate glasses. *Amer. Mineral.* **77,** 898–900.

MELANDER L. and SAUNDERS W. H. (1980) *Reaction Rates of Isotopic Molecules.* Wiley.

MORTIER W. J., SAUER J., LERCHER J. A., and NOLLER H. (1984) Bridging and terminal hydroxyls. A structural chemical and quantum chemical discussion. *J. Phys. Chem.* **88,** 905–912.

MUIER I. J., BANCROFT G. M., and NESBITT H. W. (1989) Characteristic of altered laboradorite surfaces by SIMS and XPS. *Geochim. Cosmochim. Acta* **53,** 1235–1241.

MUIR I. J. and NESBITT H. W. (1991) Effects of aqueous cations on the dissolution of labradorite feldspar. *Geochim. Cosmochim. Acta* **55,** 3181–3189.

MURPHY W. M. and HELGESON H. C. (1987) Thermodynamic and kinetic constraints on reaction rates among minerals and aqueous solutions. III Activated complexes and the pH-dependence of the rates of feldspar, pyroxene, wollastonite, and olivine hydrolysis. *Geochim. Cosmochim. Acta* **51,** 3137–3153.

NAGY K. L. and LASAGA A. C. (1992) Dissolution and precipitation of gibbsite at 80°C and pH 3: the dependence on solution saturation state. *Geochim. Cosmochim. Acta* **56,** 3903–3111.

NESBITT H. W., MACRAE N. D., and SHOTYK W. (1991) Congruent and incongruent dissolution of labradorite in dilute, acidic, salt solutions. *J. Geol.* **99,** 429–442.

NEWTON M. D. and GIBBS G. V. (1980) Ab initio calculated geometries and charge distributions for H_4SiO_4 and $H_6Si_2O_7$ compared with experimental values for silicates and siloxanes. *Phys. Chem. Mineral.* **6,** 221–246.

NICHOLAS J. B., WINANS R. E., HARRISON R. J., ITON L. E., CURTISS L. A., and HOPFINGER A. J. (1992) An ab initio investigation of

disiloxane using extended basis sets and electron correlation. *J. Phys. Chem.* **96,** 7958–7965.

POE B. T., MCMILLAN P. F., AUSTEN ANGELL C., and SATO R. K. (1992) Al and Si coordination in SiO_2—Al_2O_3 glasses and liquids: A study by NMR and IR spectroscopy and MD simulations. *Chem. Geol.* **96,** 333–349.

RIMSTIDT J. D. and BARNES H. L. (1980) The kinetics of silica-water reactions. *Geochim. Cosmochim. Acta* **44,** 1683–1699.

ROSE N. M. (1991) Dissolution rates of prenite, epidote, and albite. *Geochim. Cosmochim. Acta* **55,** 3273–3286.

SAUER J. (1987) Molecular structure of orthosilicic acid, silanol, and $H_3SiO \cdot AlH_3$ complex: Models of surface hydroxyls in silica and zeolites. *J. Phys. Chem.* **91,** 2315–2319.

SAUER J. (1989) Molecular models in ab-initio studies of solids and surfaces: from ionic crystals and semiconductors to catalysis. *Chem. Rev.* **89,** 199–255.

SAUER J. and ZAHRADNIK R. (1984) Quantum chemical studies of zeolites and silica. *Intl. J. Quantum Chem.* **26,** 793–822.

SCHWEDA P. S. (1989) Kinetics of alkali feldspar dissolution at low temperatures. In *Water-Rock Interaction,* pp. 609–612. Balkema.

SCHINDLER P. W. and STUMM W. (1987) The surface chemistry of oxides, hydroxides and oxide minerals. In *Aquatic Surface Chemistry* (ed. W. STUMM), pp. 83–110. Wiley.

STUMM W., FURRER G., WIELAND E., and ZINDER B. (1985) The effects of complex-forming ligands on the dissolution of oxides and aluminosilicates. In *The Chemistry of Weathering* (ed. J. I. DREVER), pp. 55–74. D. Reidel.

STUMM W. and MORGAN J. (1981) *Aquatic Chemistry.* Wiley.

STUMM W. and WOLLAST R. (1990) Coordination chemistry of weathering: Kinetics of the surface-controlled dissolution of oxide minerals. *Rev. Geophys.* **28,** 53–69.

TRUONG N. T. and TRUHLAR D. G. (1990) Ab initio transition state theory calculations of the reaction rate $OH + CH_4 \rightarrow H_2O + CH_3$. *J. Chem. Phys.* **93,** 1761–1769.

UGLIENGO P., SAUNDERS V., and GARRONE E. (1990) Silanol as a model for the free hydroxyl of amorphous silica: Ab initio calculations of the interaction with water. *J. Phys. Chem.* **94,** 2260–2267.

VAN HOOK W. A. (1970) Kinetic Isotope Effects: Introduction and discussion of the theory. In *Isotope Effects in Chemical Reactions* (ed. C. J. COLLINS and N. S. BOWMAN), pp. 1–89. Van Nostrand Reinhold Co.

WESTALL J. C. (1987) Adsorption mechanisms in aquetic surface chemistry. In *Aquatic Surface Chemistry* (ed. W. STUMM), pp. 3–32. Wiley.

WIELAND E., WEHRLI B., and STUMM W. (1988) The coordination chemistry of weathering: III. A generalization on the dissolution rates of minerals. *Geochim. Cosmochim. Acta* **52,** 1969–1981.

WOLLAST R. and CHOU L. (1992) Surface reactions during the early stages of weathering of albite. *Geochim. Cosmochim. Acta* **56,** 3113–3121.

XUE X., STEBBINS J. F., KANZAKI M., and TONNES R. G. (1989) Silicon coordination and speciation changes in a silicate liquid at high pressure. *Science* **245,** 962–964.

YAMABE S. and MINATO T. (1984) Ab initio calculations of the thermochemical data on the $H_3O^+ + H_2O = H_5O_2^+$ gas-phase clustering. *J. Chem. Phys.* **80,** 1576–1578.